R O S E T T A

FLIGHT REPORTS
of RPC–MAG

RO-IGEP-TR0028

Step by Step
Calibration Procedure
for RPC-MAG Data

Issue: 3 Revision: 1

May 8, 2015

Ingo Richter

e-mail: i.richter@tu-bs.de
Institut für Geophysik und extraterrestrische Physik
Technische Universität Braunschweig
Mendelssohnstraße 3, 38106 Braunschweig
Germany

Contents

1 Introduction

This document describes calibration of the RPCMAG magnetic field data. Prior to launch intensive testing and a complete calibration of the instrument has been executed at the Magnetic Coil Facility *MAGNETSRODE*, operated by the Institute for Geophysics and extraterrestrial Physics, Technische Universität Braunschweig. The principle and basic parameters obtained by this ground calibration is described in detail in section 3.

The evaluated parameters have to be applied in a well defined way to the data measured in space. The step by step procedure leading to various data products is described in section 4 and its subchapters.

2 Applicable Documents

- AD1: Richter I., Rahm M.,RO-IGM-TR-0002, Fluxgate Magnetometer Calibration for Rosetta: Report on the FM and FS Calibration Institut für Geophysik und Meteorologie, Braunschweig, Oktober 2001
- AD2: Othmer C., Richter I., RO-IGM-TR-0003, Fluxgate Magnetometer Calibration for Rosetta: Analysis of the FM Calibration Institut für Geophysik und Meteorologie, Braunschweig, Oktober 2001
- AD3: Eichelberger H., Schwingenschuh K.,Aydogar O., Baumjohann W. RO-IWF-TR0001, Calibration Report, Sample Rate and Frequency Response - Analysis of ROSETTA RPC-MAG IWF Graz, January 2002
- AD4: Richter I., RO-IGEP-TR-0007, RPC-MAG Software DDS2PDS User Manual Institut für Geophysik und extraterrestrische Physik, Braunschweig, January 2010
- AD5: Richter I., Diedrich A., Glassmeier K.H. RO-IGEP-TR-0009, EAICD, ROSETTA-RPC-MAG To Planetary Science Archive Interface Control Document Institut für Geophysik und extraterrestrische Physik, Braunschweig, June 2012
- AD6: Rosetta Mission Control System (RMCS) Data Delivery Interface Document, DDID, RO-ESC-IF-5003
- AD7: Diedrich A., Glassmeier K.-H., Richter I., RO-IGEP-TN0001, RPCMAG Internal Packet Definitions, Institut für Geophysik und extraterrestrische Physik, Technische Universität Braunschweig
- AD8: Lee C., PIU Magnetometer Processing Software Overview, RO-RPC-MA-6007
- AD9: Richter, I., Cupido E., ROSETTA PLASMA CONSORTIUM USER MANUAL, RO-RPC-UM

3 Ground Calibration

3.1 Summary

The ground calibration has been performed at the magnetic coil facility MAGNETSRODE. At this facility the magnetometers can be operated in known and stable magnetic field conditions. Artificial magnetic calibration fields can be applied in a range from -100000 nT to +100000 nT on each individual coil axis X_c, Y_c, Z_c. The accuracy of the fields is better than 0.8 nT. Additionally to these DC fields AC fields can be applied in the same range with frequencies up to the order of Kilohertz. The device under test can not only be operated at room temperature but also in wide temperature range from $-196°$C up to $+200°$C using a special designed unmagnetic thermal box. (At the time of the ROSETTA calibration only the previous generation of thermal equipment was available, allowing to change temperatures in the range $-55°$C up to $+100°$C).
The DC ground calibration comprises the determination of the following temperature dependent entities:

- Offset-Vector $\underline{B}_{\text{off}}(T)$
- Sensitivity-Matrix $\underline{\underline{\sigma}}(T)$
- Misalignment.Matrix $\underline{\underline{\omega}}(T)$

A coarse overview about the numerical values for both sensors outboard (OB) and inboard (IB) is given now:

OFFSETS:

$$\underline{B}_{\text{off,OB}}(T) = \begin{pmatrix} 214.5 \\ -79.9 \\ 384.7 \end{pmatrix} + \begin{pmatrix} -1.053 \\ 0.0730 \\ -1.6570 \end{pmatrix} \cdot T \quad [\text{nT}, \text{K}]$$

$$\underline{B}_{\text{off,IB}}(T) = \begin{pmatrix} 114.3 \\ -119.8 \\ 494 \end{pmatrix} + \begin{pmatrix} -0.565 \\ 0.731 \\ -1.673 \end{pmatrix} \cdot T \quad [\text{nT}, \text{K}]$$

SENSITIVITIES:

$$\underline{\underline{\sigma}}_{\mathrm{OB}}(T) = \begin{pmatrix} 1.091 & 0 & 0 \\ 0 & 1.09352 & 0 \\ 0 & 0 & 1.09289 \end{pmatrix} + \begin{pmatrix} -11.8 & 0 & 0 \\ 0 & -8.21 & 0 \\ 0 & 0 & -6.97 \end{pmatrix} \cdot 10^{-6} \cdot T \quad [\mathrm{nT, K}]$$

$$\underline{\underline{\sigma}}_{\mathrm{IB}}(T) = \begin{pmatrix} 1.0907 & 0 & 0 \\ 0 & 1.09434 & 0 \\ 0 & 0 & 1.09413 \end{pmatrix} + \begin{pmatrix} -14.2 & 0 & 0 \\ 0 & -9.30 & 0 \\ 0 & 0 & -8.55 \end{pmatrix} \cdot 10^{-6} \cdot T \quad [\mathrm{nT, K}]$$

MISALIGNMENT ANGLES:

$$\begin{aligned} \xi_{\mathrm{xy,OB}}(T) &= 90.0666 - 6.04 \cdot 10^{-5} \cdot T \quad [\,^{\circ}, \mathrm{K}] \\ \xi_{\mathrm{xz,OB}}(T) &= 90.0366 - 1.11 \cdot 10^{-4} \cdot T \quad [\,^{\circ}, \mathrm{K}] \\ \xi_{\mathrm{yz,OB}}(T) &= 90.0370 - 8.12 \cdot 10^{-5} \cdot T \quad [\,^{\circ}, \mathrm{K}] \end{aligned}$$

$$\begin{aligned} \xi_{\mathrm{xy,IB}}(T) &= 90.0348 + 8.54 \cdot 10^{-5} \cdot T \quad [\,^{\circ}, \mathrm{K}] \\ \xi_{\mathrm{xz,IB}}(T) &= 89.9587 + 3.71 \cdot 10^{-5} \cdot T \quad [\,^{\circ}, \mathrm{K}] \\ \xi_{\mathrm{yz,IB}}(T) &= 89.9433 + 1.20 \cdot 10^{-4} \cdot T \quad [\,^{\circ}, \mathrm{K}] \end{aligned}$$

The complete description and and background information concerning these parameters are presented in the next chapters.

3.2 Mathematical Description of the Ground Calibration

3.2.1 Basic Principle

The Magnetsrode Coil Facility (MCF) generates an artificial magnetic field $\underline{B}^c$ that can be considered as a calibrated, orthogonal magnetic reference field[a)]. The magnetometer under test at the center of the coil system (CoC) generates magnetic raw data $\underline{B}^r$. These data include an eventually existing residual field of the coil system $\underline{B}^{res}$ and the magnetometer

[a)] During the calibration the temperature dependent sensitivity of the coil system is calculated every 3 minutes and taken into account as well as the static misalignment of the coil system to produce orthogonal, known fields.

offset $\underline{B}^{off}$.

$$\underline{B}^{or} = \underline{B}^{off} + \underline{B}^{res}$$

Therefore, the first step of the calibration is the generation of offset and residual field corrected measured field data $\underline{B}^{m}$:

$$\underline{B}^{m} = \underline{B}^{r} - \underline{B}^{or}$$

The actual offset and residual field is automatically taken into account during the calibration analysis. Either a constant field or - if needed - a linear trend of $\underline{B}^{or}$ is subtracted from the raw data.

The relation between the calibration field and the magnetometer data is then defined by

$$\underline{B}^{m} = \underline{\underline{F}}\ \underline{B}^{c}$$

where $\underline{\underline{F}}$ is the complete calibration transfer matrix, defined by

$$\underline{\underline{F}} = \underline{\underline{S}}\ \underline{\underline{O}}\ \underline{\underline{R}}.$$

$\underline{\underline{S}}(T)$ represents the temperature dependent sensitivity.
$\underline{\underline{O}}(T)$ describes the temperature dependent internal sensor misalignment (orthogonalisation matrix).
$\underline{\underline{R}}(T)$ describes the rotation of the sensor against the coil axes.[b)]

The calibration algorithms compute the inverse matrices:

$$\begin{aligned} \underline{\underline{\phi}} &=: \underline{\underline{F}}^{-1} \\ &= \underline{\underline{R}}^{-1}\ \underline{\underline{O}}^{-1}\ \underline{\underline{S}}^{-1} \\ &=: \underline{\underline{\rho}}\ \underline{\underline{\omega}}\ \underline{\underline{\sigma}}\ . \end{aligned}$$

These matrices have the following shape:

$$\underline{\underline{\sigma}} = \begin{pmatrix} \sigma_1 & 0 & 0 \\ 0 & \sigma_2 & 0 \\ 0 & 0 & \sigma_3 \end{pmatrix} ,$$

$$\underline{\underline{\omega}} = \begin{pmatrix} 1 & \cos\xi_{xy} & \cos\xi_{xz} \\ 0 & \sin\xi_{xy} & \dfrac{\cos\xi_{yz} - \cos\xi_{xy}\cos\xi_{xz}}{\sin\xi_{xy}} \\ 0 & 0 & \sqrt{\sin^2\xi_{xz} - \dfrac{(\cos\xi_{yz} - \cos\xi_{xy}\cos\xi_{xz})^2}{\sin^2\xi_{xy}}} \end{pmatrix} ,$$

[b)] Also the rotation matrix is regarded as temperature dependent being able to consider any thermal setup inadequacies causing fractional rotations.

$$\underline{\underline{\rho}} = \begin{pmatrix} 1 & 0 & 0 \\ 0 & \cos\lambda & -\sin\lambda \\ 0 & \sin\lambda & \cos\lambda \end{pmatrix} \begin{pmatrix} \cos\mu & 0 & \sin\mu \\ 0 & 1 & 0 \\ -\sin\mu & 0 & \cos\mu \end{pmatrix} \begin{pmatrix} \cos\nu & -\sin\nu & 0 \\ \sin\nu & \cos\nu & 0 \\ 0 & 0 & 1 \end{pmatrix}$$

The rotation matrix $\underline{\underline{R}}$ is of interest just for the calibration to determine the right magnetometer parameters. The transfer function for the normal use of the magnetometer is just given by

$$\underline{\phi} = \underline{\underline{\omega}}\,\underline{\sigma}$$

3.2.2 Temperature Effects

In the last section the basic principle of calibrating a linear sensor has been described. Now the important question of temperature dependence shall be discussed.
Three aspects will be considered:

- Temperature influence on the OFFSET.
- Temperature influence on the SENSITIVITY.
- Temperature influence on the ALIGNMENT.

The temperature parameters were measured during the ground calibration at the Magnetsrode Coil Facility. To save some time, the two sensors IB and OB, were tested in parallel. For this purpose they were both placed in the temperature box. Thus, one sensor is fixed a few centimeters north and the other one is some centimeters south of CoC. Therefore, the calibration field acting at these positions is not the same as the reference field at CoC used for the other calibration tasks.

For this reason a special algorithm described below was developed to deduce the "true" temperature effects from the measurements with a slightly "wrong" field.

3.2.2.1 Temperature Influence on the OFFSET

Offset measurements are executed under zero field condition. Therefore, no geometrical problem, mentioned above, arises.
There are two methods to obtain the sensor offsets:

1. Assuming a properly working facility the residual field of the coil system $\underline{B}^{res}$ stays constant. This constant residual field has to be determined before the thermal measurements and must be subtracted to get the offset. The residual field determination and nulling is a standard procedure before any calibration.

   The temperature dependence of the offset can generally be computed as

   $$\underline{B}^{off}(T) = \sum_{k=0}^{n} \underline{B}_k^{off} \cdot T^k - \underline{B}^{res}$$

   The polynomial coefficients $\underline{B}_k^{off}$ are evaluated by the analysis software using a polynomial fit of zerofield measurements $\underline{B}^{off}(T_i)$ at all temperature levels T_i available.

2. A more accurate method uses the usual sensor rotations by 180° around two main axes to obtain the sensor offsets. Adding the measurement values from the normal and the turned position reveals the sensor offset

   $$\underline{B}^{off}(T_i) = \frac{\underline{B}^r_{0^\circ}(T_i) + \underline{B}^r_{180^\circ}(T_i)}{2},$$

   subtracting yields the coils system residual field:

   $$\underline{B}^{res}(t) = \frac{\underline{B}^r_{0^\circ}(t) - \underline{B}^r_{180^\circ}(t)}{2},$$

   This residual field is only time dependent and not a function of the sensor temperature. The temperature dependence of the sensor can then be determined using a polynomial fit of all complete sets of offset measurements $\underline{B}^{off}(T_i)$ at the specific temperature levels T_i:

   $$\underline{B}^{off}(T) = \sum_{k=0}^{n} \underline{B}_k^{off} \cdot T^k$$

For the ROSETTA ground calibration it was not possible to rotate the sensor by 180° whilst operated inside the temperature box. Therefore the first method had to be applied for measuring the temperature dependence of the offset. Thus the sum of offset and residual field were measured. This means that the constant residual field has to be subtracted to get the offset. It can be determined by comparing the standard offset measurements (180° sensor flipping at CoC) at the reference temperature T_1 with the "temperature offset measurement" (i.e. the offset as determined during the temperature cycle) at T_1.

Combining all this, the offsets for the ROSETTA sensors are expressed as

$$\underline{B}^{off} = \underline{a}_0 + \underline{a}_1 \cdot T$$

The fit-coefficients a_i are provided in the delivered calibration files.

3.2.2.2 Temperature Influence on the SENSITIVITY

The standard temperature model for a FGM sensor assumes a linear temperature dependence of the sensitivity. Therefore, the sensitivity components can be described as follows:

$$\sigma_i(T) = \sigma_{0,i} + \sigma_{1,i} \cdot T$$

Here $\sigma_{0,i}$ assigns the offset and $\sigma_{1,i}$ the slope of the i^{th} component of the sensitivity. Performing measurements at CoC would reveal exactly this behavior. As, however, the measurements are taken at an off–CoC position one gets a slightly different law

$$\sigma_i^1(T) = \sigma_{0,i}^1 + \sigma_{1,i}^1 \cdot T$$

where the 1 in the exponent assigns the off–CoC position.

At CoC just the reference sensitivity $\sigma_i^0(T_1)$ measured at T_1 is known (upper index 0 denotes CoC position) from an independent measurement outside the T–cycle. Thus the problem is the calculation of the temperature dependent sensitivity at CoC

$$\sigma_i^0(T) = \sigma_{0,i}^0 + \sigma_{1,i}^0 \cdot T$$

from the known coefficients.

Solution:
For the temperature T_1 the sensitivities at different places inside the coil system should only differ by a constant geometry correction factor

$$k_i = \frac{\sigma_i^1(T_1)}{\sigma_i^0(T_1)}.$$

As this factor is a temperature independent coil system parameter, $\sigma_i^0(T)$ can be deduced by

$$\sigma_i^0(T) = \frac{1}{k_i}\ \sigma_i^1(T).$$

Hence

$$\sigma_i^0(T) = \frac{1}{k_i}\ \left(\sigma_{0,i}^1 + \sigma_{1,i}^1 \cdot T\right)$$

delivers the desired result.

3.2.2.3 Temperature Influence on the ALIGNMENT

For the alignment a linear temperature dependency of the misalignment angles ξ_{xy}, ξ_{xz}, ξ_{yz} is assumed.

$$\xi_{ij}(T) = \xi_{0,ij} + \xi_{1,ij} \cdot T$$

Here $\xi_{0,ij}$ assigns the offset and $\xi_{1,ij}$ the slope of the ij–angle of the misalignment. Performing measurements at CoC would reveal exactly this behavior. As, however, the measurement are taken at an off–CoC position one gets a slightly different law

$$\xi^1_{ij}(T) = \xi^1_{0,ij} + \xi^1_{1,ij} \cdot T$$

where the 1 in the exponent assigns the off–CoC position.

At CoC just the reference angles $\xi^0_{ij}(T_1)$ measured at T_1 are known (upper limit 0 denotes CoC position) from an independent measurement. Thus the problem is the calculation of the temperature dependent angles at CoC

$$\xi^0_{ij}(T) = \xi^0_{0,ij} + \xi^0_{1,ij} \cdot T$$

from the known coefficients, or more precisely, to get the temperature dependent orthogonalisation matrix

$$(\underline{\underline{\omega^0}})(T) = \begin{pmatrix} 1 & \cos(\xi^0_{xy}(T)) & \cos(\xi^0_{xz}(T)) \\ 0 & \sin(\xi^0_{xy}(T)) & \frac{\cos(\xi^0_{yz}(T)) - \cos(\xi^0_{xy}(T)) \cdot \cos(\xi^0_{xz}(T))}{\sin(\xi^0_{xy}(T))} \\ 0 & 0 & \sqrt{\sin^2(\xi^0_{xz}(T)) - (\omega^0(1,2))^2} \end{pmatrix}$$

at CoC.

Solution:
The consideration of the sensitivity revealed a geometrical correction factor k_i which defines the transfer from off–CoC position to the CoC.
In the case of the alignment angles, however, a constant scalar factor is not the right tool to transform the angles, as these angles appear in cosine-terms of the orthogonalisation matrix. Therefore, the transformation is made by a geometrical correction matrix $\underline{\underline{K}}$ which is defined by the orthogonalisation ratio of measurements at CoC and an off–CoC position at constant temperature T_1.

$$\underline{\underline{K}} = (\underline{\underline{\omega^0}})^{-1}(T_1) \cdot (\underline{\underline{\omega^1}})(T_1)$$

As this matrix is a temperature independent coil system parameter, the desired orthogonalisation matrix $\omega^0(T)$ can be deduced by

$$(\underline{\underline{\omega^0}})(T) = (\underline{\underline{\omega^1}})(T) \cdot \underline{\underline{K}}^{-1}$$

Hence

$$(\underline{\underline{\omega^0}})(T) = \begin{pmatrix} 1 & \cos(\xi^1_{xy}(T)) & \cos(\xi^1_{xz}(T)) \\ 0 & \sin(\xi^1_{xy}(T)) & \frac{\cos(\xi^1_{yz}(T)) - \cos(\xi^1_{xy}(T)) \cdot \cos(\xi^1_{xz}(T))}{\sin(\xi^1_{xy}(T))} \\ 0 & 0 & \sqrt{\sin^2(\xi^1_{xz}(T)) - (\omega^1(1,2))^2} \end{pmatrix} \cdot \underline{\underline{K}}^{-1}$$

delivers the desired result.

3.3 Ground Calibration Coefficients

For the ROSETTA mission it was decided to fly this magnetometer configuration:

Unit	Selection
DPU	FS
IB–Sensor	FM–IB
OB–Sensor	FM–OB

Accordingly the calibration coefficients are available in the ground calibration files
`RPCMAG_001_CALIB_FSDPU_FMIB.TXT`
`RPCMAG_001_CALIB_FSDPU_FMOB.TXT`
for the Inboard and Outboard sensor operated with the Flight Spare Digital Processing unit (FSDPU) actually flying onboard ROSETTA. These files are delivered in the `CALIB` directory.

3.3.1 Final Results for the Flight IB Sensor

3.3.1.1 Offset

The sensor offset obeys the equation

$$\boxed{\underline{B}^{off} = \underline{a}_0 + \underline{a}_1 \cdot T - \underline{B}^{res}}$$

The calibration revealed:

$\underline{a}_0$ [nT]	$\underline{a}_1$ [nT/K]	$\underline{B}^{res}$ [nT]
114.3	-0.565	-2.0
-119.8	0.731	2.0
494.0	-1.673	-15.0

These coefficients are labeled A_0 and A_1 in the calibration files.

3.3.1.2 Sensitivity

Reference Temperature for Linearity/Sphere–Measurement: $T_1 = 17.39$ [°C]

Reference Sensitivities for Linearity/Sphere–Measurement at T_1 at CoC:

$\sigma^0_x(T_1)$ [1]	$\sigma^0_y(T_1)$ [1]	$\sigma^0_z(T_1)$ [1]
1.09045	1.09418	1.09398

The coefficients from the temperature calibration at the off-center position are

$\sigma^1_{0,x}$ [1]	$\sigma^1_{0,y}$ [1]	$\sigma^1_{0,z}$ [1]
1.09026	1.09354	1.09336

$\sigma^1_{1,x}$ [1/K]	$\sigma^1_{1,y}$ [1/K]	$\sigma^1_{1,z}$ [1/K]
-1.42E-005	-9.29E-006	-8.55E-006

The geometrical correction coefficient $\underline{k}$, caused by the 2 different positions during the linearity measurements and the temperature measurements is defined by

$$k_i = \frac{\sigma_i^1(T_1)}{\sigma_i^0(T_1)}$$

The evaluation reveals

k_x [1]	k_y [1]	k_z [1]
0.99959	0.99927	0.99929

Using this factor the desired temperature dependence of the sensitivity

$$\sigma_i^0(T) = \frac{1}{k_i}\left(\sigma_{0,i}^1 + \sigma_{1,i}^1 \cdot T\right)$$

can be evaluated. The needed coefficients

$$\begin{aligned} \sigma_{0,i}^0 &:= \frac{1}{k_i}\left(\sigma_{0,i}^1\right) \\ \sigma_{1,i}^0 &:= \frac{1}{k_i}\left(\sigma_{1,i}^1\right) \end{aligned}$$

for the sensitivity

$$\boxed{(S_{ii})^{-1} =: \sigma_i^0 = \sigma_{0,i}^0 + \sigma_{1,i}^0 \cdot T}$$

are:

$\sigma_{0,x}^0$ [1]	$\sigma_{0,y}^0$ [1]	$\sigma_{0,z}^0$ [1]
1.09070	1.09434	1.09413

$\sigma_{1,x}^0$ [1/K]	$\sigma_{1,y}^0$ [1/K]	$\sigma_{1,z}^0$ [1/K]
-1.42E-005	-9.30E-006	-8.55E-006

These coefficients are labeled SIGMA_00 and SIGMA_01 in the calibration files.

3.3.1.3 Alignment

Reference Temperature for Linearity/Sphere–Measurement: $T_1 = 17.39$ [°C]
Reference Misalignment for Linearity/Sphere–Measurement at T_1 at CoC:

$\xi^0_{xy}(T_1)$ [°]	$\xi^0_{xz}(T_1)$ [°]	$\xi^0_{yz}(T_1)$ [°]
90.0463	89.9416	89.9500

The alignment coefficients obtained from the temperature calibration at the off-center position are

$\xi^1_{0,xy}$ [°]	$\xi^1_{0,xz}$ [°]	$\xi^1_{0,yz}$ [°]
90.0348	89.9587	89.9433

$\xi^1_{1,xy}$ [°/K]	$\xi^1_{1,xz}$ [°/K]	$\xi^1_{1,yz}$ [°/K]
8.54E-005	3.71E-005	1.20E-004

The geometrical correction matrix $\underline{\underline{K}}$, caused by the 2 different positions during the linearity measurements and the temperature measurements is defined by

$$\underline{\underline{K}} = (\underline{\underline{\omega}}^0)^{-1}(T_1) \cdot (\underline{\underline{\omega}}^1)(T_1)$$

with the inverse misalignment matrix $\underline{\underline{\omega}} =: \underline{\underline{O}}^{-1}$, consisting of the direction cosines $\cos(\xi_{ij})$. The evaluation reveals

$$\boxed{(\underline{\underline{K}})^{-1} = \begin{pmatrix} 1.00000 & -0.00017 & 0.00031 \\ 0.00000 & 1.00000 & -0.00008 \\ 0.00000 & 0.00000 & 1.00000 \end{pmatrix}}$$

Using this matrix the desired temperature dependence of the alignment

$$\boxed{(\underline{\underline{\omega}}^0)(T) = (\underline{\underline{\omega}}^1)(T) \cdot \underline{\underline{K}}^{-1}}$$

can be evaluated. $(\underline{\underline{\omega^0}})(T)$ results as

$$\boxed{(\underline{\underline{\omega}}^0)(T) = \begin{pmatrix} 1 & \cos(\xi^1_{xy}(T)) & \cos(\xi^1_{xz}(T)) \\ 0 & \sin(\xi^1_{xy}(T)) & \frac{\cos(\xi^1_{yz}(T)) - \cos(\xi^1_{xy}(T)) \cdot \cos(\xi^1_{xz}(T))}{\sin(\xi^1_{xy}(T))} \\ 0 & 0 & \sqrt{\sin^2(\xi^1_{xz}(T)) - (\omega^1(1,2))^2} \end{pmatrix} \begin{pmatrix} 1.00000 & -0.00017 & 0.00031 \\ 0.00000 & 1.00000 & -0.00008 \\ 0.00000 & 0.00000 & 1.00000 \end{pmatrix}}$$

with

$$\boxed{\xi^1_{ij}(T) = \xi^1_{0,ij} + \xi^1_{1,ij} \cdot T}$$

These coefficients are labeled XI_10 and XI_11 in the calibration files. The elements of the $\underline{\underline{K}}^{-1}$ matrix are labeled K_0, K_1, and K_2.

3.3.2 Final Results for the Flight OB Sensor

3.3.2.1 Offset

The sensor offset obeys the equation

$$\boxed{\underline{B}^{off} = \underline{a}_0 + \underline{a}_1 \cdot T - \underline{B}^{res}}$$

The calibration revealed:

$\underline{a}_0$ [nT]	$\underline{a}_1$ [nT/K]	$\underline{B}^{res}$ [nT]
214.5	-1.053	0.0
-79.9	0.073	4.0
384.7	-1.657	-20.0

These coefficients are labeled A_0 and A_1 in the calibration files.

3.3.2.2 Sensitivity

Reference Temperature for Linearity/Sphere–Measurement: $T_1 = 17.39$ [°C]

Reference Sensitivities for Linearity/Sphere–Measurement at T_1 at CoC:

$\sigma_x^0(T_1)$ [1]	$\sigma_y^0(T_1)$ [1]	$\sigma_z^0(T_1)$ [1]
1.09079	1.09338	1.09277

The coefficients from the temperature calibration at the off-center position are

$\sigma_{0,x}^1$ [1]	$\sigma_{0,y}^1$ [1]	$\sigma_{0,z}^1$ [1]
1.09066	1.09251	1.09217

$\sigma_{1,x}^1$ [1/K]	$\sigma_{1,y}^1$ [1/K]	$\sigma_{1,z}^1$ [1/K]
-1.18E-005	-8.20E-006	-6.97E-006

The geometrical correction coefficient $\underline{k}$, caused by the 2 different positions during the linearity measurements and the temperature measurements is defined by

$$k_i = \frac{\sigma_i^1(T_1)}{\sigma_i^0(T_1)}$$

The evaluation reveals

k_x [1]	k_y [1]	k_z [1]
0.99969	0.99907	0.99934

Using this factor the desired temperature dependence of the sensitivity

$$\sigma_i^0(T) = \frac{1}{k_i}\left(\sigma_{0,i}^1 + \sigma_{1,i}^1 \cdot T\right)$$

can be evaluated. The needed coefficients

$$\begin{aligned} \sigma_{0,i}^0 &:= \frac{1}{k_i}\left(\sigma_{0,i}^1\right) \\ \sigma_{1,i}^0 &:= \frac{1}{k_i}\left(\sigma_{1,i}^1\right) \end{aligned}$$

for the sensitivity

$$\boxed{(S_{ii})^{-1} =: \sigma_i^0 = \sigma_{0,i}^0 + \sigma_{1,i}^0 \cdot T}$$

are:

$\sigma_{0,x}^0$ [1]	$\sigma_{0,y}^0$ [1]	$\sigma_{0,z}^0$ [1]
1.09100	1.09352	1.09289

$\sigma_{1,x}^0$ [1/K]	$\sigma_{1,y}^0$ [1/K]	$\sigma_{1,z}^0$ [1/K]
-1.18E-005	-8.21E-006	-6.97E-006

These coefficients are labeled SIGMA_00 and SIGMA_01 in the calibration files.

3.3.2.3 Alignment

Reference Temperature for Linearity/Sphere–Measurement: $T_1 = 17.39$ [°C]
Reference Misalignment for Linearity/Sphere–Measurement at T_1 at CoC:

$\xi^0_{xy}(T_1)$ [°]	$\xi^0_{xz}(T_1)$ [°]	$\xi^0_{yz}(T_1)$ [°]
90.0711	90.0187	90.0576

The alignment coefficients obtained from the temperature calibration at the off-center position are

$\xi^1_{0,xy}$ [°]	$\xi^1_{0,xz}$ [°]	$\xi^1_{0,yz}$ [°]
90.0666	90.0366	90.0370

$\xi^1_{1,xy}$ [°/K]	$\xi^1_{1,xz}$ [°/K]	$\xi^1_{1,yz}$ [°/K]
-6.04E-005	-1.11E-004	-8.12E-005

The geometrical correction matrix $\underline{\underline{K}}$, caused by the 2 different positions during the linearity measurements and the temperature measurements is defined by

$$\underline{\underline{K}} = (\underline{\underline{\omega}}^0)^{-1}(T_1) \cdot (\underline{\underline{\omega}}^1)(T_1)$$

with the inverse misalignment matrix $\underline{\underline{\omega}} =: \underline{\underline{O}}^{-1}$, consisting of the direction cosines $\cos(\xi_{ij})$. The evaluation reveals

$$\boxed{(\underline{\underline{K}})^{-1} = \begin{pmatrix} 1.00000 & -0.00010 & 0.00028 \\ 0.00000 & 1.00000 & -0.00038 \\ 0.00000 & 0.00000 & 1.00000 \end{pmatrix}}$$

Using this matrix the desired temperature dependence of the alignment

$$\boxed{(\underline{\underline{\omega}}^0)(T) = (\underline{\underline{\omega}}^1)(T) \cdot \underline{\underline{K}}^{-1}}$$

can be evaluated. $(\underline{\underline{\omega}}^0)(T)$ results as

$$\boxed{(\underline{\underline{\omega}}^0)(T) = \begin{pmatrix} 1 & \cos(\xi^1_{xy}(T)) & \cos(\xi^1_{xz}(T)) \\ 0 & \sin(\xi^1_{xy}(T)) & \frac{\cos(\xi^1_{yz}(T)) - \cos(\xi^1_{xy}(T)) \cdot \cos(\xi^1_{xz}(T))}{\sin(\xi^1_{xy}(T))} \\ 0 & 0 & \sqrt{\sin^2(\xi^1_{xz}(T)) - (\omega^1(1,2))^2} \end{pmatrix} \begin{pmatrix} 1.00000 & -0.00010 & 0.00028 \\ 0.00000 & 1.00000 & -0.00038 \\ 0.00000 & 0.00000 & 1.00000 \end{pmatrix}}$$

with

$$\boxed{\xi^1_{ij}(T) = \xi^1_{0,ij} + \xi^1_{1,ij} \cdot T}$$

These coefficients are labeled XI_10 and XI_11 in the calibration files. The elements of the $\underline{\underline{K}}^{-1}$ matrix are labeled K_0, K_1, and K_2.

3.3.3 Calibration of the Sensor Thermistors

The sensor temperatures are measured using standard PT1000 thermistors inside the sensors. Table 1 shows a part of the manufacturer's provided nominal function derived from the following third order polynomial functions $T(U)$.

$$T(U) = c_0 \; + \; c_1 U \; + \; c_2 U^2 \; + \; c_3 U^3$$

with

c_0= -368.61072
c_1= 458.49304
c_2= -356.02890
c_3= 180.00644

T [°C]	R(T) [Ω]	U(T) [V]	T [°C]	R(T) [Ω]	U(T) [V]
-150.000	423.219	0.743420	10.0000	1039.14	1.27399
-140.000	461.402	0.789310	20.0000	1078.40	1.29715
-130.000	499.567	0.832850	30.0000	1117.77	1.31951
-120.000	537.730	0.874230	40.0000	1157.26	1.34112
-110.000	575.906	0.913610	50.0000	1196.86	1.36201
-100.000	614.108	0.951160	60.0000	1236.58	1.38222
-90.0000	652.351	0.987000	70.0000	1276.41	1.40178
-80.0000	690.646	1.02128	80.0000	1316.36	1.42072
-70.0000	729.005	1.05408	90.0000	1356.43	1.43907
-60.0000	767.436	1.08552	100.000	1396.60	1.45686
-50.0000	805.950	1.11569	110.000	1436.90	1.47411
-40.0000	844.555	1.14466	120.000	1477.31	1.49084
-30.0000	883.256	1.17251	130.000	1517.84	1.50708
-20.0000	922.061	1.19931	140.000	1558.48	1.52286
-10.0000	960.974	1.22512	150.000	1599.24	1.53818
0.000000	1000.00	1.25000			

Table 1: Calibration data for the sensor PT1000 thermistor, nominal data provided by the manufacturer.

Therefore, the raw temperature T_s^r of sensor s (s={IB | OB}), measured in [e°C], is obtained by applying the polynomial coefficients to the sensor output voltage.

$$\begin{aligned} T^r_{\mathrm{IB}}(U_{\mathrm{T,IB}}) &= c_0 + c_1 U_{\mathrm{T,IB}} + c_2 U^2_{\mathrm{T,IB}} + c_3 U^3_{\mathrm{T,IB}} \\ T^r_{\mathrm{OB}}(U_{\mathrm{T,OB}}) &= c_0 + c_1 U_{\mathrm{T,OB}} + c_2 U^2_{\mathrm{T,OB}} + c_3 U^3_{\mathrm{T,OB}} \end{aligned}$$

The temperature calibration at Magnetsrode revealed that the following temperature offsets have to be considered to get the calibrated temperature data T_s^c in °C.

$$\begin{aligned} T^O_{\mathrm{IB}} &= -1.5\ ^\circ\mathrm{C} \\ T^O_{\mathrm{OB}} &= -2.7\ ^\circ\mathrm{C} \end{aligned}$$

$$\begin{aligned} T^c_{\mathrm{IB}} &= T^r_{\mathrm{IB}} - T^O_{\mathrm{IB}} \\ T^c_{\mathrm{OB}} &= T^r_{\mathrm{OB}} - T^O_{\mathrm{OB}} \end{aligned}$$

In the calibration file the polynomial coefficients c_i are labeled T_0, T_1, T_2, T_3 and the thermistor offset correction $T^O_{\mathrm{IB,OB}}$ is denoted T_OFF.

4 Step by Step Processing of measured Flight Data

In the last section it was described how the parameters characterizing a fluxgate sensor were obtained. The present section shows now in detail how these parameters and additional entities have to be applied to convert the received binary telemetry data from the s/c into scientific usable data of various levels. The data products themselves and the differences between the levels are described in the AD5.

4.1 Generation of EDITED Raw Data

The ROSETTA s/c transmits the binary data from the RPC-MAG instrument via the RPC-PIU, the OBDH, the HGA, and deep space antennae to the DDS at ESOC were the data are stored in binary format. That format is described in AD6,AD7, and AD9.

These binary data are input of the RPCMAG RAW2ASCII s/w which converts the binary data into human readable ASCII data. This conversion from binary to ASCII data is straight forward according to the packet definitions described in AD6, AD7, and AD9 and not subject of the document in hand.

After the conversion Housekeeping (HK) and science data are available in the format of ADC counts. Magnetic field data are given in individual instrument coordinates. The relation between these individual unit reference frames (URF) of each sensor wrt. the s/c coordinates is defined in the `RPCMAG_SC_ALIGN.TXT` file to be found in the `CALIB` directory as well as in the latest version of the SPICE frame kernel file `ROS_Vnn.TF` to be found on the ESA server (nn denotes the current version of the file).

4.1.1 Housekeeping Data

The following data are available:

Data	Description
TIME_UTC	UTC TIME OF OBSERVATION: YYYY-MM-DDTHH:MM:SS.FFFFFF
TIME_OBT	S/C CLOCK AT OBSERVATION TIME, SECONDS SINCE 00:00 AT 1.1.2003: SSSSSSSSS.FFFFF
T_OB	TEMPERATURE OF THE RPCMAG OUTBOARD SENSOR. VALUE IS GIVEN IN ADC_COUNTS
T_IB	TEMPERATURE OF THE RPCMAG INBOARD SENSOR. VALUE IS GIVEN IN ADC_COUNTS
STAGE_A_ID	FILTER TYPE IDENTIFICATION FLAG A
STAGE_B_ID	FILTER TYPE IDENTIFICATION FLAG B
FILTER_CFG	FILTER CONFIGURATION FLAG
MAG_REF_VOLTAGE	MAGNETOMETER REFERENCE VOLTAGE: 2.5 V. VALUE IS GIVEN IN ADC_COUNTS
MAG_NEG_VOLTAGE	MAGNETOMETER NEGATIVE SUPPLY VOLTAGE:-5V. VALUE IS GIVEN IN ADC_COUNTS
MAG_POS_VOLTAGE	MAGNETOMETER POSITIVE SUPPLY VOLTAGE:+5V. VALUE IS GIVEN IN ADC_COUNTS
BX_OB	MAGNETIC FIELD X COMPONENT, UNCALIBRATED RAW DATA, INSTRUMENT COORDINATES, OB-SENSOR VALUE IS GIVEN IN 16 BIT ADC_COUNTS
BY_OB	MAGNETIC FIELD Y COMPONENT, UNCALIBRATED RAW DATA, INSTRUMENT COORDINATES, OB-SENSOR. VALUE IS GIVEN IN 16 BIT ADC_COUNTS
BZ_OB	MAGNETIC FIELD Z COMPONENT, UNCALIBRATED RAW DATA, INSTRUMENT COORDINATES, OB-SENSOR. VALUE IS GIVEN IN 16 BIT ADC_COUNTS

These HK data are not needed for the calibration of science data. They only provide auxiliary information about the instrument status.

4.1.2 Science Data

The following data are available:

Data	Description
TIME_UTC	UTC TIME OF OBSERVATION: YYYY-MM-DDTHH:MM:SS.FFFFFF
TIME_OBT	S/C CLOCK AT OBSERVATION TIME, SECONDS SINCE 00:00 AT 1.1.2003: SSSSSSSSS.FFFFF
BX_OB	MAGNETIC FIELD X COMPONENT, UNCALIBRATED RAW DATA, INSTRUMENT COORDINATES, OB-SENSOR. VALUE IS GIVEN IN 20 BIT ADC_COUNTS
BY_OB	MAGNETIC FIELD Y COMPONENT, UNCALIBRATED RAW DATA, INSTRUMENT COORDINATES, OB-SENSOR. VALUE IS GIVEN IN 20 BIT ADC_COUNTS
BZ_OB	MAGNETIC FIELD Z COMPONENT, UNCALIBRATED RAW DATA, INSTRUMENT COORDINATES, OB-SENSOR. VALUE IS GIVEN IN 20 BIT ADC_COUNTS
T_OB	TEMPERATURE OF THE RPCMAG OUTBOARD SENSOR. VALUE IS GIVEN IN ADC_COUNTS
T_IB	TEMPERATURE OF THE RPCMAG INBOARD SENSOR. VALUE IS GIVEN IN ADC_COUNTS
QUALITY	THE DATA QUALITY IS CODED FOR EACH VECTOR. CODE: 0= GOOD DATA; 1= BAD DATA EACH SENSOR HAS ITS OWN QUALITY BIT BIT0:X, BIT1:Y,BIT2:Z, BIT3=0:OB, BIT3=1 IB

4.2 Generation of LEVEL_A Data

The LEVEL_A data are the first step of calibrated data. LEVEL_A HK data are directly obtained from the EDITED RAW by application of the nominal conversion algorithm to convert ADC counts to physical values.

LEVEL_A Science data also take the ground calibration, temperature effects and a specific timeshift into account. Finally data are available in instrument coordinates.

4.2.1 General remarks concerning the conversion of digital values

RPCMAG contains seven 20bit ADCs. 3 are used for the digitalization of magnetic field data measured by the OB sensor, 3 are used for the magnetic field data of the IB sensor, and the seventh, which is operated with a multiplexer, converts various Housekeeping (HK) data. The reference voltage of the ADCs is 2.5 V. The converters are operated in a bipolar mode, thus input voltages in the range of ±2.5V can be converted. The relation of input voltage and counts is:

$$\begin{aligned} 00000\text{h} &\iff -2.5\text{V} \\ 80000\text{h} &\iff 0V \\ \text{FFFFFh} &\iff +2.5\text{V} \end{aligned}$$

Due to the small input range some voltage adaption has to be done in the MAG instrument for certain HK values:

- the 2.5V reference voltage is monitored behind a voltage divider 100016Ω/(100000Ω+100016Ω)=0.499 as 1.2497 V nominal voltage.
- the +5V supply voltage is monitored behind a voltage divider 90956Ω/(99972Ω+90956Ω)=0.476 as 2.38V nominal voltage.
- the -5V supply voltage is monitored behind a voltage divider 27400Ω/(100024Ω+27400Ω)=0.215 as -0.997 V nominal voltage.
- the temperatures are measured as the voltage drop of PT1000 thermistors connected to the 2.5V reference voltage via a 1kΩ serial resistor:

$$U(T) = U_{ref} \cdot \frac{1}{\frac{R_{ser}}{R(T)} + 1}$$

Therefore, the nominal voltages at 273 K are 1.25 V. Conversion to temperatures are obtained by application of 3rd order polynomials.

RPCMAG sends always 20bit data to the PIU. The PIU reduces the amount of data in the following way:

Science data:

Data	PIU-Input	PIU-Output	PIU-Operation
Magnetic field IB	20 bit	20 bit	subtract 2^{19}
Magnetic field OB	20 bit	20 bit	subtract 2^{19}

Housekeeping data:

Data	PIU-Input	PIU-Output	PIU-Operation
Magnetic field OB	20bit	16bit	subtract 2^{19} right shift by 4 digits
2.5V Ref. Voltage	20bit	20bit	subtract 2^{19}
+5V Supply Voltage	20bit	8bit	subtract 2^{19} skip highest 4bits subtract offset 79F7h right shift by 4 digits
-5V Supply Voltage	20bit	8bit	subtract 2^{19} skip highest 4bits subtract offset -370Eh right shift by 3 digits
Temperature OB	20bit	16bit	subtract 2^{19} right shift by 4 digits
Temperature IB	20bit	16bit	subtract 2^{19} right shift by 4 digits

4.2.2 Housekeeping Data

4.2.2.1 Nominal Conversion of ADC Counts to Physical Housekeeping Data: Magnetic Field Values

Housekeeping magnetic field data are available as 16 Bit values. The operational range is ±16384 nT.

Definitions:

$$\begin{aligned} B_{MAX} &= +16384\text{nT} \\ B_{MIN} &= -16384\text{nT} \\ COUNTS16 &= 2^{16} = 65536 \\ NOMINAL_{FACTOR} &= \frac{B_{MAX} - B_{MIN}}{COUNTS16 - 1} \end{aligned}$$

The TLM data contain 16bit data. The relation between the ADCvalues and the PIU output (TLM) is:

$$TLM = (ADCvalue - 2^{19}) \;\; shr \; 4$$

The data range of these TLM data is 0...+counts16-1. The decimal representation of these unsigned integers are the EDITED RAW HK DATA. Unit is [counts].

In the first step of the conversion to physical values an offset of $\frac{counts16}{2}$ is added if the value is smaller than $\frac{counts16}{2}$ and subtracted in the other case. The nominal relation between these $CONVERTED\_DATA$ and magnetic field is now as follows:

$$\begin{aligned} \text{0000h} &\Longleftrightarrow B_{MIN} \\ \text{8000h} &\Longleftrightarrow 0 \\ \text{FFFFh} &\Longleftrightarrow B_{MAX} \end{aligned}$$

To convert these values into uncalibrated [engineering, enT] nanotesla values, the following algorithm has to be applied:

$$B = Converted\_Data * Nominal\_Factor + B_{min} \;\; [enT]$$

4.2.2.2 Nominal Conversion of ADC Counts to Physical Housekeeping Data: Reference Voltage

Housekeeping data contain the values of the ADC reference voltage, available as 20 Bit values. The nominal value is 2.5 V. The typical real monitored voltage of the ADC, behind a voltage divider, is 1.2497V.

Definitions:

$$\begin{aligned} U_{MAX} &= +2.5\text{V} \\ U_{MIN} &= -2.5\text{V} \\ COUNTS20 &= 2^{20} = 1048576 \\ VOLT\_DIVIDER &= 100016/200016 = 0.49996 \\ NOMINAL\_FACTOR &= \frac{U_{max} - U_{min}}{counts20 - 1} \end{aligned}$$

The TLM data contain 20bit data. The relation between the ADCvalues and the PIU output (TLM) is:

$$TLM = (ADCvalue - 2^{19})$$

The data range of these TLM data is 0...+counts20-1. The decimal representation of these unsigned integers are the EDITED RAW HK DATA. Unit is [counts].

In the first step of the conversion to physical values an offset of $\frac{counts20}{2}$ is added if the value is smaller than $\frac{counts20}{2}$ and subtracted in the other case. The nominal relation between these converted data and magnetic field is now as follows:

$$\begin{aligned} \text{0000h} &\Longleftrightarrow U_{MIN} \\ \text{8000h} &\Longleftrightarrow 0 \\ \text{FFFFh} &\Longleftrightarrow U_{MAX} \end{aligned}$$

To convert these values into voltages the following algorithm has to be applied:

$$U_{REF} = \frac{converted\_data * Nominal\_Factor + U_{min}}{volt\_divider} \text{ [V]}$$

4.2.2.3 Nominal Conversion of ADC Counts to Physical Housekeeping Data: Positive Supply Voltage

Housekeeping data contain the values of the positve supply voltage, available as 8 Bit values. The nominal value is +5.0 V. The typical real monitored voltage of the ADC, behind a voltage divider, is 2.38V.

Definitions:

$$\begin{aligned} U_{MAX} &= +2.5\text{V} \\ U_{MIN} &= -2.5\text{V} \\ U_{REF} &= +2.4996\text{V} \\ U_{CENTER} &= +5.0\text{V} \\ COUNTS8 &= 2^8 = 256 \\ VOLT\_DIVIDER &= 90956/(99972 + 90956) = 0.476389 \\ CAL\_FACTOR &= \frac{U_{ref}}{(counts20 - 1) \cdot volt\_divider} \cdot 512 = 0.002562 \end{aligned}$$

The TLM data contain 8bit data. The relation between the ADCvalues and the PIU output (TLM) is:

$$TLM = ((((ADCvalue - 2^{19}) \ \ shr\ 4) - 79F7h) \ \ shr\ 4)$$

The data range of these TLM data is 0...+counts8-1. The decimal representation of these unsigned integers are the EDITED RAW HK DATA. Unit is [counts].

In the first step of the conversion to physical values these unsigned integer TLM values are converted to signed integers, thus an offset of counts8 is subtracted if the value is greater than $\frac{counts8}{2}$. The nominal relation between these converted data and the original voltage is now as follows:

80h	=	-128d	$\Longleftrightarrow$	4.673 V
00h	=	0d	$\Longleftrightarrow$	5.00 V
7Fh	=	127d	$\Longleftrightarrow$	5.327 V

To convert these values into voltages, the following algorithm has to be applied:

$$U+ = cal\_fak \cdot converted\_data + U_{center}\ [\text{V}]$$

4.2.2.4 Nominal Conversion of ADC Counts to Physical Housekeeping Data: Negative Supply Voltage

Housekeeping data contain the values of the negative supply voltage, available as 8 Bit values. The nominal value is −5.0 V. The typical real monitored voltage of the ADC, behind a voltage divider, is 0.997V.

Definitions:

$$\begin{aligned} U_{MAX} &= +2.5\text{V} \\ U_{MIN} &= -2.5\text{V} \\ U_{REF} &= +2.4996\text{V} \\ U_{CENTER} &= -5.0\text{V} \\ COUNTS8 &= 2^8 = 256 \\ VOLT\_DIVIDER &= 27400/(100024 + 27400) = 0.21503 \\ CAL\_FACTOR &= \frac{U_{ref}}{(counts20 - 1) \cdot volt\_divider} \cdot 256 = 0.002838 \end{aligned}$$

The TLM data contain 8bit data. The relation between the ADCvalues and the PIU output (TLM) is:

$$TLM = ((((ADCvalue - 2^{19}) \ \ shr\ 4) + 370Eh) \ \ shr\ 3)$$

The data range of these TLM data is 0...+counts8-1. The decimal representation of these unsigned integers are the EDITED RAW HK DATA. Unit is [counts].

In the first step of the conversion to physical values these unsigned integer TLM values are converted to signed integers, thus an offset of counts8 is subtracted if the value is greater than $\frac{counts8}{2}$. The nominal relation between these converted data and the original voltage is now as follows:

80h	=	-128d	$\Longleftrightarrow$	-5.36 V
00h	=	0d	$\Longleftrightarrow$	-5.00 V
7Fh	=	127d	$\Longleftrightarrow$	-4.64 V

To convert these values into voltages, the following algorithm has to be applied:

$$U+ = cal\_fak \cdot converted\_data + U_{center} \text{ [V]}$$

4.2.2.5 Nominal Conversion of ADC Counts to Physical Housekeeping Data: Sensor Temperatures

Housekeeping data contain the values of the sensor temperatures, available as 16 Bit values. The temperature range is of the sensors is $-200°C \ldots +200°C$, according to ADC input voltages of 0.5V ... 1.6V.

Definitions:

$$\begin{aligned} U_{MAX} &= +2.5\text{V} \\ U_{MIN} &= -2.5\text{V} \\ COUNTS16 &= 2^{16} = 65536 \\ NOMINAL\_FACTOR &= \frac{U_{max} - U_{min}}{counts16 - 1} \end{aligned}$$

The TLM data contain 16bit data. The relation between the ADCvalues and the PIU output (TLM) is:

$$TLM = (ADCvalue - 2^{19}) \;\; shr \; 4$$

The data range of these TLM data is 0...+counts16-1. The decimal representation of these unsigned integers are the EDITED RAW HK DATA. Unit is [counts].

In the first step of the conversion to physical values an offset of counts16/2 is added to the TLM data.

To convert these values into voltages, the following algorithm has to be applied:

$$U(T) = (TLM\_data + \frac{counts16}{2}) \cdot Nominal\_Factor + U_{min} \; [V]$$

The calibrated temperatures can be derived from these voltages by application of a 3rd order calibration polynomial:

$$T = T_0 + T_1 * U(T) + T_2 * U^2(T) + T_3 * U^3(T)$$

The coefficients T_i are:

$$\begin{aligned} T_0 &= -368.6107 \\ T_1 &= +458.4930 \\ T_2 &= -356.0289 \\ T_3 &= +180.0064 \end{aligned}$$

4.2.2.6 Data Availability

The following data are available after application of the conversion algorithms described in the last two section:

Data	Description
TIME_UTC	UTC TIME OF OBSERVATION: YYYY-MM-DDTHH:MM:SS.FFFFFF
TIME_OBT	S/C CLOCK AT OBSERVATION TIME, SECONDS SINCE 00:00 AT 1.1.2003: SSSSSSSSS.FFFFF
T_OB	TEMPERATURE OF THE RPCMAG OUTBOARD SENSOR. VALUE IS GIVEN IN KELVIN
T_IB	TEMPERATURE OF THE RPCMAG INBOARD SENSOR. VALUE IS GIVEN IN KELVIN
STAGE_A_ID	FILTER TYPE IDENTIFICATION FLAG A
STAGE_B_ID	FILTER TYPE IDENTIFICATION FLAG B
FILTER_CFG	FILTER CONFIGURATION FLAG
MAG_REF_VOLTAGE	MAGNETOMETER REFERENCE VOLTAGE: 2.5 V. VALUE IS GIVEN IN VOLT
MAG_NEG_VOLTAGE	MAGNETOMETER NEGATIVE SUPPLY VOLTAGE:-5V. VALUE IS GIVEN IN VOLT
MAG_POS_VOLTAGE	MAGNETOMETER POSITIVE SUPPLY VOLTAGE:+5V. VALUE IS GIVEN IN VOLT
BX_OB	MAGNETIC FIELD X COMPONENT, UNCALIBRATED RAW DATA, INSTRUMENT COORDINATES, OB-SENSOR VALUE IS GIVEN IN NANOTESLA
BY_OB	MAGNETIC FIELD Y COMPONENT, UNCALIBRATED RAW DATA, INSTRUMENT COORDINATES, OB-SENSOR. VALUE IS GIVEN IN NANOTESLA
BZ_OB	MAGNETIC FIELD Z COMPONENT, UNCALIBRATED RAW DATA, INSTRUMENT COORDINATES, OB-SENSOR. VALUE IS GIVEN IN NANOTESLA

4.2.3 Science Data

The generation of LEVEL_A Science data is performed in the following steps:

1. Eliminate all EDITED RAW data vectors which are labeled as bad (i.e a problem occurred during the transmission in one or more components). Every vector containing a QUALITY flag $\neq 0$ will not be used.
2. Transform all remaining the EDITED RAW data (ADC counts) to physical values. This is done using the nominal conversion procedure described in section 4.2.3.1.
3. Apply the results of the ground calibration. Refer to section 4.2.3.2.
4. Calculate the right offset from the extended temperature model. Refer to section 4.2.3.3.
5. Apply right time shift according to actual Filter Mode. Refer to section 4.2.3.5.

4.2.3.1 Nominal Conversion of ADC Counts to Physical Science Data: Magnetic Field Values

Scientific magnetic field data are digitized with 20 Bit. The operational range is ±15000 nT.
Definitions:

$$\begin{aligned} B_{MAX} &= +15000 \text{ nT} \\ B_{MIN} &= -15000 \text{ nT} \\ COUNTS &= 2^{20} = 1048576 \\ NOMINAL\_FACTOR &= \frac{B_{MAX} - B_{MIN}}{COUNTS - 1} \end{aligned}$$

The TLM data contain signed 20bit data. The data range of these values in decimal representation is $-\frac{counts20}{2} \ldots + \frac{counts20}{2} - 1$. These signed integers are the EDITED RAW DATA. Unit is [counts].
In the first step of conversion to physical values an offset of $\frac{counts20}{2}$ is added, which yields to data in the range of 00000h:FFFFFh. The nominal relation between these converted TLM data and magnetic field is now as follows:

$$\begin{aligned} \text{00000h} &\iff B_{MIN} \\ \text{80000h} &\iff 0 \\ \text{FFFFFh} &\iff B_{MAX} \end{aligned}$$

To convert these data into uncalibrated [engineering, enT] nanotesla values, the following algorithm has to be applied:

$$B = [TLMdata + \frac{counts20}{2}] \cdot Nominal\_Factor + B_{min}\ [enT]$$

4.2.3.2 Application of Ground Calibration Results

1. Calibrate the sensor temperatures (ref. to section 3.3.3):

$$\begin{aligned} T^c_{\mathrm{IB}}(U_{\mathrm{T,IB}}) &= c_0 + c_1 U_{\mathrm{T,IB}} + c_2 U^2_{\mathrm{T,IB}} + c_3 U^3_{\mathrm{T,IB}} - T^O_{\mathrm{IB}} \\ T^c_{\mathrm{OB}}(U_{\mathrm{T,OB}}) &= c_0 + c_1 U_{\mathrm{T,OB}} + c_2 U^2_{\mathrm{T,OB}} + c_3 U^3_{\mathrm{T,OB}} - T^O_{\mathrm{OB}} \end{aligned}$$

   The voltages $U_{\mathrm{T,IB}}$, and $U_{\mathrm{T,OB}}$ are the thermistor EDITED RAW data T_IB and T_OB. from the data file.

2. Calculate the actual, temperature dependent sensor offset (cf. sections 3.3.1.1, 3.3.2.1):

$$B^{off}_{s,i} = a_{s,0} + a_{s,1} \cdot T^c_s$$

3. Generate the offset corrected magnetic field raw data:

$$B^m_{s,i} = B^r_{s,i} - B^{off}_{s,i}$$

   The $B^r_{s,i}$ values are the converted magnetic field raw data from the last subsection.

4. Calculate the actual, temperature dependent sensitivity (cf. sections 3.3.1.2, 3.3.2.2):

$$(S_{s,ii})^{-1}(T) =: \sigma^0_{s,i}(T) = \sigma^0_{0,s,i} + \sigma^0_{1,s,i} \cdot T^c_s$$

5. Evaluate the temperature dependent sensor misalignment (cf. sections 3.3.1.3, 3.3.2.3):

$$\underline{\underline{O}}^{-1}_s(T) =: \underline{\underline{\omega}}^0_s(T) = \begin{pmatrix} 1 & \cos(\xi^0_{xy}(T)) & \cos(\xi^0_{xz}(T)) \\ 0 & \sin(\xi^0_{xy}(T)) & \frac{\cos(\xi^0_{yz}(T)) - \cos(\xi^0_{xy}(T)) \cdot \cos(\xi^0_{xz}(T))}{\sin(\xi^0_{xy}(T))} \\ 0 & 0 & \sqrt{\sin^2(\xi^0_{xz}(T)) - (\omega^0(1,2))^2} \end{pmatrix}$$

6. Apply calibration matrices to produce calibrated data:

$$\begin{aligned} \underline{B}^c_s &= \underline{\underline{O}}^{-1}_s(T)\ \underline{\underline{S}}^{-1}_s(T)\ \underline{B}^m_s \\ &= \underline{\underline{\omega}}^{(}_s T)\ \underline{\sigma}_s(T)\ \underline{B}^m_s \end{aligned}$$

4.2.3.3 Offset Calculation using the Extended Temperature Model

During flight the range of the temperature calibration performed on ground in an interval between -70°C ... +70° C turned out to be not broad enough. For the lowest temperature measured at the sensor until end of 2009 was about -140°C. Therefore, a new temperature model (finally we ended up at model 006) was created using the inflight data of calm (according to magnetic field conditions) mission phases. For the sensitivity and the alignment the original linear model derived from the ground calibration is sufficient, but the offset behavior needs to be treated a little more detailed for the extended temperature range. Thus, the inflight magnetic field data are compared with the temperature data and fitted against the temperature by the means of a 3rd order polynomial $P_3(T)$. To improve the quality and to diminish hysteretic effects these additional polynomials are evaluated individually for every day. The polynomial coefficients $p_{s,k,i}$ (sensor s, order k, component i) are stored in the daily calibration files `RPCMAG_yymmdd_006_CALIB_IB.TXT` and `RPCMAG_yymmdd_006_CALIB_OB.TXT`. For the reason of a flexible handling of any possibly occurring temperature effect these files contain sets of six parameters ($\rightsquigarrow$ 5th order polynomials) although usually are only polynomials up to 3rd order are used. All higher coefficients which are not taken into account are set to zero, thus they do not have any impact on the computed polynomials.

The improvement of the temperature dependency of the sensor offset is done is the following way:
The original ground calibrated data $\underline{B}_s^c$ (cf. item 6 in section 4.2.3.2) has to be transformed as

$$\underline{B}_s^{c,new} = \underline{B}_s^c - \underline{B}_{off,s}^{new}.$$

Here

$$B_{\mathrm{off,s,i}}^{new}(\tilde{T}_\mathrm{s}) = p_{0,s,i} \; + \; p_{1,s,i}\tilde{T}_\mathrm{s} \; + \; p_{2,s,i}\tilde{T}_\mathrm{s}^2 \; + \; p_{3,s,i}\tilde{T}_\mathrm{s}^3$$

describes the polynomial fit of the offset–temperature behavior. As temperature the reduced temperature $\tilde{T} = T_s - T_s^O$ has to be used.

After alle these operations, which have to be performed for every individual vector with the actual parameters, the offset behavior is modelled almost sufficiently. At last it just has to be ensured that no artificial magnetic field jumps occur at the midnight time – this might happen as the data are processed on a daily base and different days have different calibration files. To get rid of any jump the specific calculated offset values at the end of a day are stored in a separate file and taken into account to adjust a possible offset jump at midnight. The data of the following day will be shifted in that way that a possible midnight jump disappears. This only applies for a joint measurement campaign over a few days. If subsequent measurements are interrupted by more than a few hours an offset-jump adaption is neither needed nor used.

4.2.3.4 Offset Calculation for Phases after the Hibernation

After the end of hibernation in 2014 and the "commissioning after hibernation" the magnetometer was operating quasi permanently. For the first time in the mission this offered the opportunity to collect long time series of magnetic field data and learning a lot about the spacecraft and the other payload. From all the measurements during summer 2014 we learned that the s/c is very dirty in terms of magnetic properties. Lots of "magnetic noise" at various time scales is generated. On the low frequency side of the time scales there are signatures of various switched currents flowing on the s/c and also of thrusters being operated. Also other payload is probably generating magnetic disturbances. However, due to the complexity of the system it is hardly possible to distinguish between all the sources. We made the attempt to investigate about 200 s/c HK parameters and to analyse their impact on the magnetic field time series. There are some correlations but unfortunately there is currently no possibility to write robust and fool proof s/w to eliminate all these disturbances.
Furthermore it turned out, that the assumed temperature effects seen in the previous phases of short measurements (due to limited operation time) up to 2011, proved to be probably only slightly temperature dependent sensor offset drifts but mainly changes of the s/c magnetic field caused by s/c current changes, attitude changes, thruster operations, etc. Taking all that into consideration it turned out, that an high order temperature model up to 5th order polynomials is not the right means to improve the DC component of the magnetic field data. It worthwhile mentioning again, that not the sensor offset is causing problems, but the varying s/c field!
Therefore, we took the data of summer 2014 and adjusted the DC-levels (time dependent) that way, that the B_z-component of the magnetic field (in CSEQ-coordinates) becomes zero — at the long term average. This is compatible with the usual long term solar wind properties. Furthermore the offset components in s/c-coordinates (CLB,CLF-data) were adjusted that way, that any impact of a s/c-rotation was minimized in the CSEQ-coordinates (CLC, CLG-data). For a s/c generated magnetic field, visible in s/c-coordinates as shifted DC-level, acts like a rotating dipole, if – due to all the pointing requirements – the s/c has to be rotated. Thus, argumentum e contrario if there is no correlation between the s/c rotation and the magnetic field signature –represented in CSEQ-coordinates– the sum of sensor offsets and s/c field is balancing the DC level of the magnetic field – represented in s/c-coordinates – to zero. This method would work perfectly if attitude changes would cover 360° in two orthogonal planes. Unfortunately the pointing changes were much smaller, and therefore, the mentioned algorithm in deed improves the magnetic field DC values but does not adjust them perfectly.
Due to the high level of s/c activity and lots of uncertainties it was not possible to clean the time series completely but to gain significant improvement in comparison to any different method else applied to our data.
Appendix B lists the relevant lines of the correction algorithm and presents the offsets that have been applied to the LEVEL B data at certain times in order to minimize visibility of rotational effects visible in CSEQ - data.

4.2.3.5 Application of Filter Mode dependent Time Shifts

Finally the timestamps of the measured data have to be adjusted. As the data are filtered by a mode dependent digital filter (refer to AD8 for details) the data are delayed for a certain amount of time. The timeshift was first recognized at the first Earth swing by, where the magnetic field data measured were in nearly perfect accordance to the magnetic field model of the Earth - except a tiny time shift of a few seconds. This behavior was later proofed and tested with the FGM spare unit at Imperial College. The theoretical timeshifts - verified by this test - are compiled in the following table. The shifts are valid for the actual primary sensor, which is usually the OB sensor. The table shows the times to be added to the time stamp of the vector to get the real physical event time:

SID	Mode Name	Packet Length [s]	Time to add to PRIMARY data timestamp [s]
SID1	Minimum	1024	223.7
SID2	Normal	32	8.2
SID3	Burst	16	0
SID4	Medium	32	1.35
SID5	Low	128	27.7
SID6	Test	16	0

For the SECONDARY vectors the situation is different as these vectors are not filtered but just picked out of the data stream. The following table applies for the time shift of the SECONDARY vectors.

SID	Mode Name	Packet Length [s]	Time to add to SECONDARY data timestamp [s]
SID1	Minimum	1024	1023.95
SID2	Normal	32	31.95
SID3	Burst	16	15.95
SID4	Medium	32	31.95
SID5	Low	128	127.95

At this stage the data processing for generation calibrated LEVEL_A data in Instrument coordinates is complete. The created data files contain the following entities:

Data	Description
TIME_UTC	UTC TIME OF OBSERVATION: YYYY-MM-DDTHH:MM:SS.FFFFFF
TIME_OBT	S/C CLOCK AT OBSERVATION TIME, SECONDS SINCE 00:00 AT 1.1.2003: SSSSSSSSS.FFFFF
BX	MAGNETIC FIELD X COMPONENT, CALIBRATED DATA, TEMPERATURE CORRECTED, INSTRUMENT COORDINATES VALUE IS GIVEN IN NANOTESLA
BY	MAGNETIC FIELD Y COMPONENT, CALIBRATED DATA, TEMPERATURE CORRECTED, INSTRUMENT COORDINATES VALUE IS GIVEN IN NANOTESLA
BZ	MAGNETIC FIELD Z COMPONENT, CALIBRATED DATA, TEMPERATURE CORRECTED, INSTRUMENT COORDINATES VALUE IS GIVEN IN NANOTESLA
T	TEMPERATURE OF THE RPCMAG SENSOR. VALUE IS GIVEN IN KELVIN
QUALITY	QUALITY FLAG, cf. EAICD chapter 3.3

4.3 Generation of LEVEL_B Data

4.3.1 Rotation from Instrument Coordinates to s/c–Coordinates

At the next stage the calibrated data in instrument coordinates (URF, in uvw-coordinates) have to be rotated to s/c-coordinates. This operation is defined by a fixed rotation, specific for the IB and OB sensor. The rotation matrices have been measured on ground at the ESTEC cleanroom using an optical measurement system for determination the mounting angles of the sensor wrt. the stowed and deployed boom orientations. The coefficients of the rotation matrices $\underline{\underline{R_{UVW2SC}}}$ are stored in the `RPCMAG_SC_ALIGN.TXT` file located in the `CALIB` directory. The desired magnetic field is given by:

$$\begin{aligned} \underline{B}^{IB}_{s/c} &= \underline{\underline{R_{UVW2SC}}}^{IB}\ \underline{B}^{IB}_{URF} \\ \underline{B}^{OB}_{s/c} &= \underline{\underline{R_{UVW2SC}}}^{OB}\ \underline{B}^{OB}_{URF} \end{aligned}$$

After this operation the data are available in s/c-coordinates, called LEVEL_B data.

Data	Description
TIME_UTC	UTC TIME OF OBSERVATION: YYYY-MM-DDTHH:MM:SS.FFFFFF
TIME_OBT	S/C CLOCK AT OBSERVATION TIME, SECONDS SINCE 00:00 AT 1.1.2003: SSSSSSSSS.FFFFF
BX	MAGNETIC FIELD X COMPONENT, CALIBRATED DATA, TEMPERATURE CORRECTED, S/C-COORDINATES VALUE IS GIVEN IN NANOTESLA
BY	MAGNETIC FIELD Y COMPONENT, CALIBRATED DATA, TEMPERATURE CORRECTED, S/C-COORDINATES VALUE IS GIVEN IN NANOTESLA
BZ	MAGNETIC FIELD Z COMPONENT, CALIBRATED DATA, TEMPERATURE CORRECTED, S/C-COORDINATES VALUE IS GIVEN IN NANOTESLA
T	TEMPERATURE OF THE RPCMAG SENSOR. VALUE IS GIVEN IN KELVIN
QUALITY	QUALITY FLAG, cf. EAICD chapter 3.3

4.4 Generation of LEVEL_C Data

4.4.1 Rotation from s/c–Coordinates to Celestial Coordinates

For a meaningful interpretation of the magnetic field data, a dynamic rotation from s/c-coordinates to a celestial coordinate system is needed. As ROSETTA is a deep space mission the ECLIPJ2000 frame [c)] was chosen as a convenient celestial coordinate system. The ECLIPJ2000 frame is related to the Equinox of the EPOCH J2000. It is a righthanded system with X pointing from the Sun to Vernal Equinox, Y perpendicular to X in the ecliptic plane, and Z perpendicular to the ecliptic plane, pointing up.

The rotation from s/c–coordinates

$$\begin{aligned} \underline{B}^{IB}_{ECLIP} &= \underline{\underline{R_{SC2ECLIP}}}(t,\underline{r})\ \underline{B}^{IB}_{s/c} \\ \underline{B}^{OB}_{ECLIP} &= \underline{\underline{R_{SC2ECLIP}}}(t,\underline{r})\ \underline{B}^{OB}_{s/c} \end{aligned}$$

to the ECLIPJ2000 frame is dependent on time and location of ROSETTA as the spacecraft changes its attitude along its trajectory. To calculate the rotation matrices two possibilities are available. Historically this was done using the OASW (orbit and attitude s/w) and the right ATNR (nominal Attitude files) and ORER, ORHR, ORMR,... file (Trajectory position files wrt. the SUN, EARTH, MARS,...) provided by ESA FDT (flight dynamics team). During the proceeding mission also SPICE kernels for ROSETTA were available, which make it much easier to evaluate the right position and orientation of ROSETTA. Currently the basic transformation to ECLIPJ2000 coordinates is done with the OASW library of ESA, while all further analysis of the ROSETTA data is performed using the powerful SPICE routines.

Update 2014: All geometric calculations are now performed using the SPICE system. Furthermore the standard coordinate system for the LEVEL C data is the CSEQ-system, as this is the only one, which takes the plasma-physical symmetry properties concerning Sun, Solar wind, and Comet into account.

[c)] Starting from the ECLIPJ2000 frame it is easy to transform the data any coordinate system reasonable for a specific mission phase, e.g. GSE-, MSO-, CSO-, CSEQ-coordinates. This can be done by application of the right SPICE kernel and the SPICE transformation routines widely available for all major programming languages.

After the described rotation the data are available in ECLIPJ2000/CSEQ coordinates, called LEVEL_C data.

Data	Description
TIME_UTC	UTC TIME OF OBSERVATION: YYYY-MM-DDTHH:MM:SS.FFFFFF
TIME_OBT	S/C CLOCK AT OBSERVATION TIME, SECONDS SINCE 00:00 AT 1.1.2003: SSSSSSSSS.FFFFF
POSITION_X	SPACECRAFT POSITION, X COMPONENT, ECLIPJ2000/CSEQ VALUE IS GIVEN IN KILOMETER
POSITION_Y	SPACECRAFT POSITION, Y COMPONENT, ECLIPJ2000/CSEQ VALUE IS GIVEN IN KILOMETER
POSITION_Z	SPACECRAFT POSITION, Z COMPONENT, ECLIPJ2000/CSEQ VALUE IS GIVEN IN KILOMETER
BX	MAGNETIC FIELD X COMPONENT, CALIBRATED DATA, TEMPERATURE CORRECTED, ECLIPJ2000/CSEQ-COORDINATES VALUE IS GIVEN IN NANOTESLA
BY	MAGNETIC FIELD Y COMPONENT, CALIBRATED DATA, TEMPERATURE CORRECTED, ECLIPJ2000/CSEQ-COORDINATES VALUE IS GIVEN IN NANOTESLA
BZ	MAGNETIC FIELD Z COMPONENT, CALIBRATED DATA, TEMPERATURE CORRECTED, ECLIPJ2000/CSEQ-COORDINATES VALUE IS GIVEN IN NANOTESLA
QUALITY	QUALITY FLAG, cf. EAICD chapter 3.3

4.5 Generation of LEVEL_D Data

The LEVEL_D data product does not exist anymore. The analysis s/w is just capable to generate so called LEVEL_D plots which show the differences between the OB and IB timeseries. Regarding the calibration, LEVEL_D plots do not play any role.

4.6 Generation of LEVEL_E Data

LEVEL_E data are averaged CALIBRATED LEVEL_A data. The data are averaged in the time domain and represent the magnetic field in instrument coordinates. LEVEL_E data are usually not generated in the standard archive process. The average is calculated in the following way. All data within a given average interval of n seconds are summed up and divided by the number of data in this interval. The timetag of such a newly averaged data point is the time of the middle of the regarded average interval.

The following data are available as LEVEL_E data.

Data	Description
TIME_UTC	UTC TIME OF OBSERVATION: YYYY-MM-DDTHH:MM:SS.FFFFFF
TIME_OBT	S/C CLOCK AT OBSERVATION TIME, SECONDS SINCE 00:00 AT 1.1.2003: SSSSSSSSS.FFFFF
BX	MAGNETIC FIELD X COMPONENT, CALIBRATED DATA, TEMPERATURE CORRECTED, INSTRUMENT-COORDINATES, 1s AVERAGE, VALUE IS GIVEN IN NANOTESLA
BY	MAGNETIC FIELD Y COMPONENT, CALIBRATED DATA, TEMPERATURE CORRECTED, INSTRUMENT-COORDINATES, 1s AVERAGE, VALUE IS GIVEN IN NANOTESLA
BZ	MAGNETIC FIELD Z COMPONENT, CALIBRATED DATA, TEMPERATURE CORRECTED, INSTRUMENT-COORDINATES, 1s AVERAGE, VALUE IS GIVEN IN NANOTESLA
QUALITY	QUALITY FLAG, cf. EAICD chapter 3.3

4.7 Generation of LEVEL_F Data

LEVEL_F data are averaged LEVEL_B or - in case of heater disturbance - LEVEL_K data. The data are averaged in the time domain and represent the magnetic field in s/c-coordinates. LEVEL_F data are generated in the standard archive process with an average interval of one second. The average is calculated in the following way. All data within a given average interval of 1s are summed up and divided by the number of data in this interval. The timetag of such a newly averaged data point is the time of the middle of the regarded average interval.

The following data are available as LEVEL_F data.

Data	Description
TIME_UTC	UTC TIME OF OBSERVATION: YYYY-MM-DDTHH:MM:SS.FFFFFF
TIME_OBT	S/C CLOCK AT OBSERVATION TIME, SECONDS SINCE 00:00 AT 1.1.2003: SSSSSSSSS.FFFFF
BX	MAGNETIC FIELD X COMPONENT, CALIBRATED DATA, TEMPERATURE CORRECTED, S/C-COORDINATES, 1s AVERAGE VALUE IS GIVEN IN NANOTESLA
BY	MAGNETIC FIELD Y COMPONENT, CALIBRATED DATA, TEMPERATURE CORRECTED, S/C-COORDINATES, 1s AVERAGE VALUE IS GIVEN IN NANOTESLA
BZ	MAGNETIC FIELD Z COMPONENT, CALIBRATED DATA, TEMPERATURE CORRECTED, S/C-COORDINATES, 1s AVERAGE VALUE IS GIVEN IN NANOTESLA
QUALITY	QUALITY FLAG, cf. EAICD chapter 3.3

4.8 Generation of LEVEL_G Data

LEVEL_G data are averaged LEVEL_C or - in case of heater disturbance - LEVEL_L data. The data are averaged in the time domain and represent the magnetic field in ECLIPJ2000-coordinates. LEVEL_G data are generated in the standard archive process with an average interval of one second. The average is calculated in the following way. All data within a given average interval of 1s are summed up and divided by the number of data in this interval. The timetag of such a newly averaged data point is the time of the middle of the regarded average interval.

The following data are available as LEVEL_G data.

Data	Description
TIME_UTC	UTC TIME OF OBSERVATION: YYYY-MM-DDTHH:MM:SS.FFFFFF
TIME_OBT	S/C CLOCK AT OBSERVATION TIME, SECONDS SINCE 00:00 AT 1.1.2003: SSSSSSSSS.FFFFF
POSITION_X	SPACECRAFT POSITION, X COMPONENT, ECLIPJ2000/CSEQ VALUE IS GIVEN IN KILOMETER
POSITION_Y	SPACECRAFT POSITION, Y COMPONENT, ECLIPJ2000/CSEQ VALUE IS GIVEN IN KILOMETER
POSITION_Z	SPACECRAFT POSITION, Z COMPONENT, ECLIPJ2000/CSEQ VALUE IS GIVEN IN KILOMETER
BX	MAGNETIC FIELD X COMPONENT, CALIBRATED DATA, TEMPERATURE CORRECTED, ECLIPJ2000/CSEQ-COORDINATES, 1s-AVERAGE, VALUE IS GIVEN IN NANOTESLA
BY	MAGNETIC FIELD Y COMPONENT, CALIBRATED DATA, TEMPERATURE CORRECTED, ECLIPJ2000/CSEQ-COORDINATES, 1s-AVERAGE, VALUE IS GIVEN IN NANOTESLA
BZ	MAGNETIC FIELD Z COMPONENT, CALIBRATED DATA, TEMPERATURE CORRECTED, ECLIPJ2000/CSEQ-COORDINATES, 1s-AVERAGE, VALUE IS GIVEN IN NANOTESLA
QUALITY	QUALITY FLAG, cf. EAICD chapter 3.3

4.9 Generation of LEVEL_H Data

LEVEL_H data are Reaction wheel (RW) and LAP disturbance corrected data. As input the LEVEL_C or — in case of heater disturbed data — LEVEL_L data are taken. Thus the data represent the magnetic field in ECLIPJ2000 coordinates.

During the ROSETTA mission the reaction wheels, which control the attitude of the s/c, turned out to create also a magnetic disturbance signature. The dynamically changing rotation frequencies of the four wheels cause AC disturbances of the magnetic field data. They occur not at the original rotation frequencies but they are folded down into the measurement frequency range according to the Nyquist sampling theorem. Thus it is an effect of aliasing. The disturbance is in the order of about 1 nanotesla and can be eliminated, as the reaction wheel frequencies are known at any time. Elimination is only reasonable for the primary sensor data in MEDIUM mode (5 vectors/s) and BURST mode (20 vectors/s) as only here the disturbance emerges significantly from the background signal/noise.

Besides this tests revealed that also the LAP instrument generates disturbances of fixed but mode dependent disturbances lines in the frequency spectrum. These lines will be eliminated by the reaction wheel disturbance purging algorithm as well. Data generation Procedure:

- Provide the Reaction wheel frequency data from the DDS (binary coded) or the Imperial college data server (SCHK7.TXT files, ASCII)
- For each time needed you have to calculate the measurement mode dependent disturbance frequency, which will occur in the data. This has to be done according to the folding theorem and the actual used sampling- and resulting Nyquist frequency.
- Fourier-Transform the magnetic field data into the frequency domain and generate a dynamic spectrum (day by day).
- For each time interval localize the 4 actual disturbed frequencies in the spectrum. In stripes of width Δf around the regarded local frequencies f the amplitudes have to be set to the values which occur in the original spectrum just below or above the regarded stripe. Add some appropriate noise to the substituted amplitudes. After having processed all data in this way, the originally clearly identifiable disturbance lines should not be visible anymore. Instead of them the slightly noisy values of the neighborhood of those lines should substitute them and only the background should be visible.
- The LAP disturbance is eliminated in a similar way: LAP generates horizontal lines in the frequency spectrum (constant frequency). The elimination is done by substituting the actual amplitudes of these line (i.e a stripe of width Δf around this lines) by the noisy background value.

- Fourier-transform the dynamic spectrum back to the time domain to create the purged time series of LEVEL_H data.

Remark: All the MAG data processing, inclusive the the RW signature correction algorithm works on a daily base. Thus all data (primary sensor) available for a specific day are processed in one instance. The main trick to get rid of the disturbing RW signatures is to operate in frequency domain rather than in time domain. The transformations into frequency domain and back to time domain are executed by a complex FFT and an inverse complex FFT respectively. After several attempts of achieving the best results it turned out, that the pure FFTs without any extra windowing gave the best results. As we were not interested in further use of the calculated spectra but just wanted to ensure having a lossless pair of transformations available, we just did it this way. We tested this pure pair of transformations and came to the conclusion that the data transition between consecutive days stays smooth and does not generate any phase problems.
Every day is separated into several time intervals of 1024 data points each. These intervals overlap by 25 % to ensure a reasonable coverage and a stable phase transition at the edges of the single time intervals. The complete set of all FF-transformed data in all these time intervals yield the dynamic spectrum of a single day which can then be purged from the occurring reaction wheel signatures by the means described above. The width Δf of the manipulated frequency band around the disturbed freq f is chosen automatically in dependence of the instrument sampling frequency. For Burst mode we use $\Delta f = 0.06$ Hz. The bandwidth values have been empirically determined, to result in the cleanest spectra. An optical inspection of each purged spectrum, reveals any possibly problems left and provides finally confidence to the used method.

The following data are available as LEVEL_H data.

Data	Description
TIME_UTC	UTC TIME OF OBSERVATION: YYYY-MM-DDTHH:MM:SS.FFFFFF
TIME_OBT	S/C CLOCK AT OBSERVATION TIME, SECONDS SINCE 00:00 AT 1.1.2003: SSSSSSSSS.FFFFF
POSITION_X	SPACECRAFT POSITION, X COMPONENT, ECLIPJ2000/CSEQ VALUE IS GIVEN IN KILOMETER
POSITION_Y	SPACECRAFT POSITION, Y COMPONENT, ECLIPJ2000/CSEQ VALUE IS GIVEN IN KILOMETER
POSITION_Z	SPACECRAFT POSITION, Z COMPONENT, ECLIPJ2000/CSEQ VALUE IS GIVEN IN KILOMETER
BX	MAGNETIC FIELD X COMPONENT, CALIBRATED DATA; TEMPERATURE, REACTION WHEEL AND LAP DISTURBANCE CORRECTED; ECLIPJ2000/CSEQ-COORDINATES, VALUE IS GIVEN IN NANOTESLA
BY	MAGNETIC FIELD Y COMPONENT, CALIBRATED DATA; TEMPERATURE, REACTION WHEEL AND LAP DISTURBANCE CORRECTED; ECLIPJ2000/CSEQ-COORDINATES, VALUE IS GIVEN IN NANOTESLA
BZ	MAGNETIC FIELD Z COMPONENT, CALIBRATED DATA; TEMPERATURE, REACTION WHEEL AND LAP DISTURBANCE CORRECTED; ECLIPJ2000/CSEQ-COORDINATES, VALUE IS GIVEN IN NANOTESLA
QUALITY	QUALITY FLAG, cf. EAICD chapter 3.3

4.10 Generation of LEVEL_I Data

LEVEL_I data are averaged LEVEL_H data. The data are averaged in the time domain and represent the magnetic field in ECLIPJ2000/CSEQ-coordinates. LEVEL_I data are not generated in the standard archive process. The average is calculated in the following way. All data within a given average interval of 1s are summed up and divided by the number of data in this interval. The timetag of such a newly averaged data point is the time of the middle of the regarded average interval.

The following data are available as LEVEL_I data.

Data	Description
TIME_UTC	UTC TIME OF OBSERVATION: YYYY-MM-DDTHH:MM:SS.FFFFFF
TIME_OBT	S/C CLOCK AT OBSERVATION TIME, SECONDS SINCE 00:00 AT 1.1.2003: SSSSSSSSS.FFFFF
POSITION_X	SPACECRAFT POSITION, X COMPONENT, ECLIPJ2000/CSEQ VALUE IS GIVEN IN KILOMETER
POSITION_Y	SPACECRAFT POSITION, Y COMPONENT, ECLIPJ2000/CSEQ VALUE IS GIVEN IN KILOMETER
POSITION_Z	SPACECRAFT POSITION, Z COMPONENT, ECLIPJ2000/CSEQ VALUE IS GIVEN IN KILOMETER
BX	MAGNETIC FIELD X COMPONENT, CALIBRATED DATA; TEMPERATURE, REACTION WHEEL AND LAP DISTURBANCE CORRECTED; ECLIPJ2000/CSEQ-COORDINATES, VALUE IS GIVEN IN NANOTESLA, 1s-AVERAGE
BY	MAGNETIC FIELD Y COMPONENT, CALIBRATED DATA; TEMPERATURE, REACTION WHEEL AND LAP DISTURBANCE CORRECTED; ECLIPJ2000/CSEQ-COORDINATES, VALUE IS GIVEN IN NANOTESLA, 1s-AVERAGE
BZ	MAGNETIC FIELD Z COMPONENT, CALIBRATED DATA; TEMPERATURE, REACTION WHEEL AND LAP DISTURBANCE CORRECTED; ECLIPJ2000/CSEQ-COORDINATES, VALUE IS GIVEN IN NANOTESLA 1s-AVERAGE
QUALITY	QUALITY FLAG, cf. EAICD chapter 3.3

4.11 Generation of LEVEL_J Data

This level is intended to contain magnetic field data which have been transformed by a Principal component analysis (PCA). The result would be three file :

- A file with the correlated contribution of OB and IB sensor, representing the external magnetic field.
- A file with the uncorrelated contribution of the OB sensor, representing the s/c noise at the location of the OB sensor.
- A file with the uncorrelated contribution of the IB sensor, representing the s/c noise at the location of the IB sensor.

As input for the PCA average LEVEL_G or LEVEL_I (in case of heater disturbance) data are taken.

The creation of LEVEL_J data is not part of the standard data archive generation process.

4.12 Generation of LEVEL_K Data

During the first Earth Swing by it happened that the ROSETTA LANDER tested some heaters which were driven by pulse width modulated square wave currents producing magnetic field disturbance signatures in the order of 0.5 nT - 1.5 nT at the location of the RPCMAG OB sensor[d)].

There are two methods for the heater signature elimination:

- An automatic elimination - using only RPCMAG data:
  METHOD1 (cf. chapter 4.12.1)
- A manual elimination - deriving the disturbed times from ROMAP data:
  METHOD2 (cf. chapter 4.12.2)

[d)] The Lander magnetometer ROMAP was disturbed by these currents in the order of 1000nT - 2000 nT

After the successful heater disturbance elimination the purged data are available in s/c-coordinates, called LEVEL_K data.

Data	Description
TIME_UTC	UTC TIME OF OBSERVATION: YYYY-MM-DDTHH:MM:SS.FFFFFF
TIME_OBT	S/C CLOCK AT OBSERVATION TIME, SECONDS SINCE 00:00 AT 1.1.2003: SSSSSSSSS.FFFFF
BX	MAGNETIC FIELD X COMPONENT, CALIBRATED DATA, TEMPERATURE CORRECTED, S/C-COORDINATES,HEATER DISTURBANCE ELIMINATED, VALUE IS GIVEN IN NANOTESLA
BY	MAGNETIC FIELD Y COMPONENT, CALIBRATED DATA, TEMPERATURE CORRECTED, S/C-COORDINATES,HEATER DISTURBANCE ELIMINATED, VALUE IS GIVEN IN NANOTESLA
BZ	MAGNETIC FIELD Z COMPONENT, CALIBRATED DATA, TEMPERATURE CORRECTED, S/C-COORDINATES,HEATER DISTURBANCE ELIMINATED, VALUE IS GIVEN IN NANOTESLA
T	TEMPERATURE OF THE RPCMAG SENSOR. VALUE IS GIVEN IN KELVIN
QUALITY	QUALITY FLAG, cf. EAICD chapter 3.3

4.12.1 Heater Disturbance Elimination: Method 1

This section investigates the impact of the Lander heaters - measured at ESB1 - to the MAG OB sensor and presents an automatic method to eliminate these disturbances.

Figure 1 shows a randomly chosen interval (March 3, 00:00 — 24:00) of RPCMAG OB data. On the first view these data look like proper magnetic field data. If we, however, zoom into the data, as done for randomly chosen interval of 30 minutes, we can clearly identify a disturbing signal in shape of a square wave with a period of T=30 s. The amplitude is not constant, but appearing with different levels. This is related to different kind of heaters (respective different currents) located on the Lander.

This disturbed signal in the B_x, B_y, B_z components (ECLIPJ2000–coordinates) is redisplayed in Figure 2. As it is easier to perform a convenient signal processing on one component with a clearly disturbed signal rather than on three slightly disturbed ones, the idea arose to turn the measured magnetic field signal into a minimum variance system. The result of this preprocessing transformation can be impressively seen in Figure 3. The complete disturbance is now superimposed on the B_x signal whereas the B_y and B_z components in the Minimum variance system are completely purged.

The real processing is visualized in Figure 4. The most upper panels shows the preprocessed data rotated into the B_x component of the minimum variance system (which is here actually the component with the maximum variance.)
The second panel shows the detection of the jumps. This is done using a moving variance indicator. A short time variance of just a few samples is evaluated and shifted step by step over the whole times series (dark blue curve). As result strong positive peaks occur at the times of the jumps, and a nearly flat signal dominates the other times. In a second step a threshold (light blue line) has to be defined to distinguish between jumps and "normal" data. Everything below this threshold belongs to "true" data, everything above this threshold is interpreted as jump caused by the heaters.
The third panel shows the separated step in the B_x time series. The times of the jumps and intermediate values are cut out.

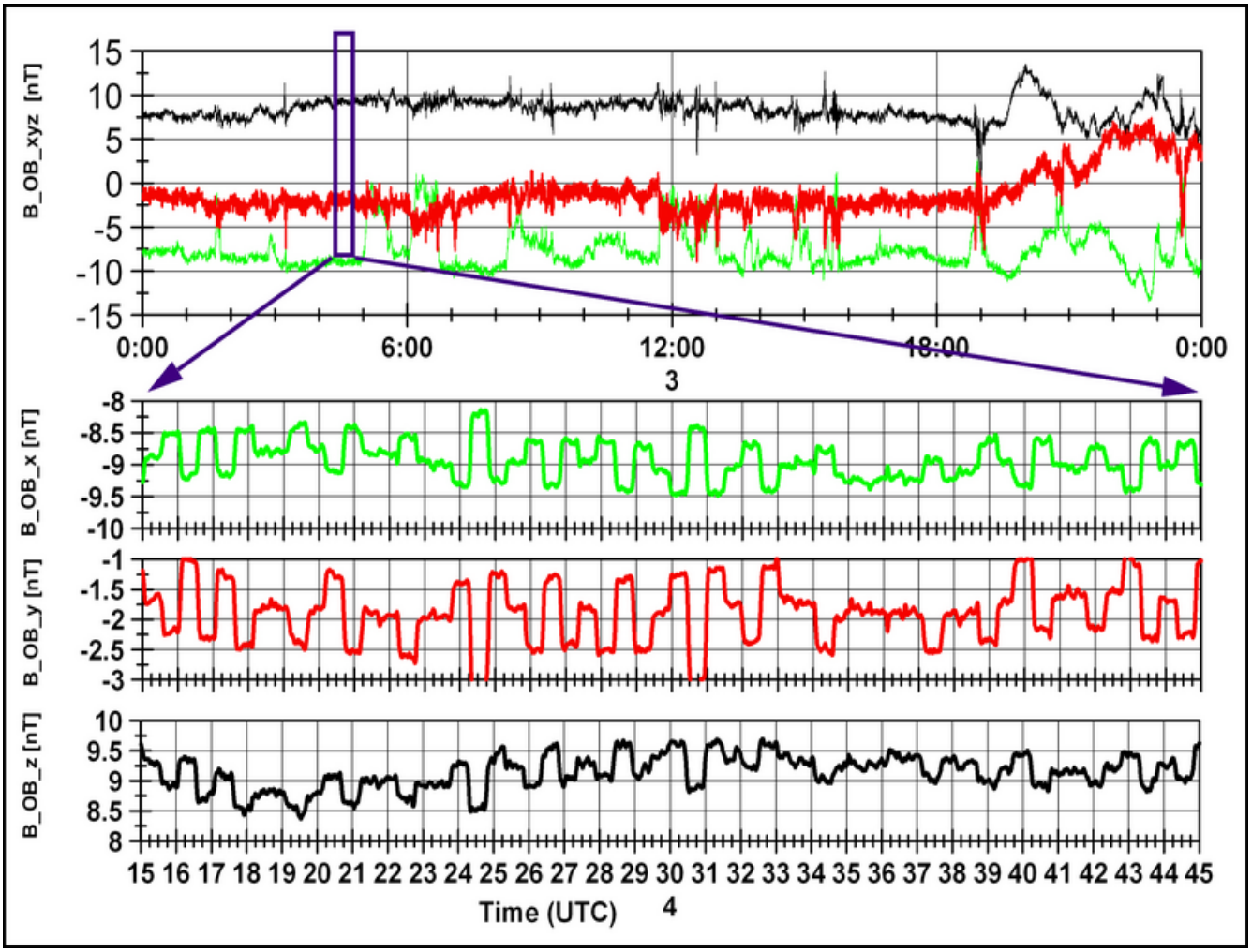

Figure 1: Original and zoomed Signal of March 3 (ECLIPJ2000).

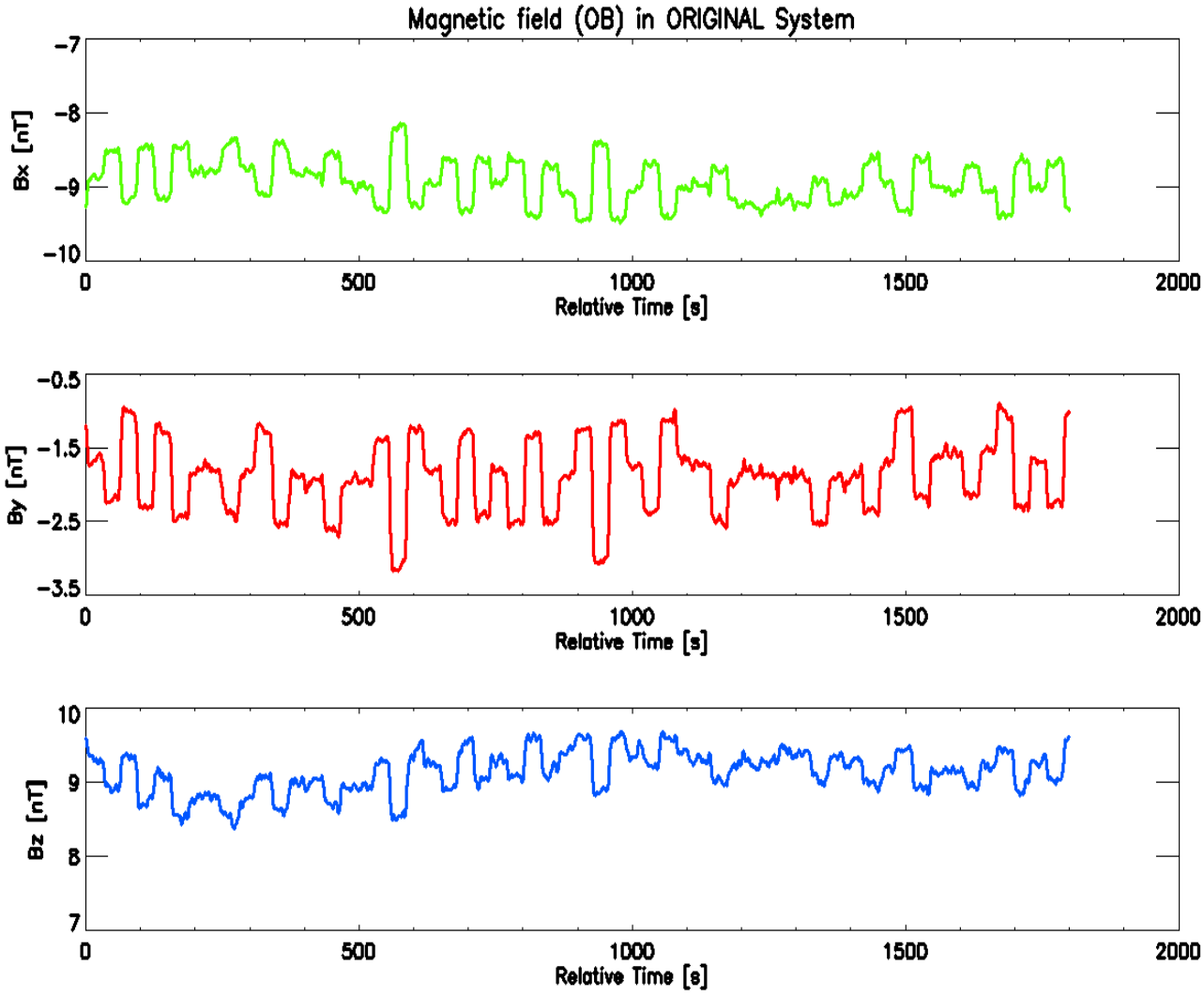

Figure 2: Original Signal disturbed by the LANDER heaters

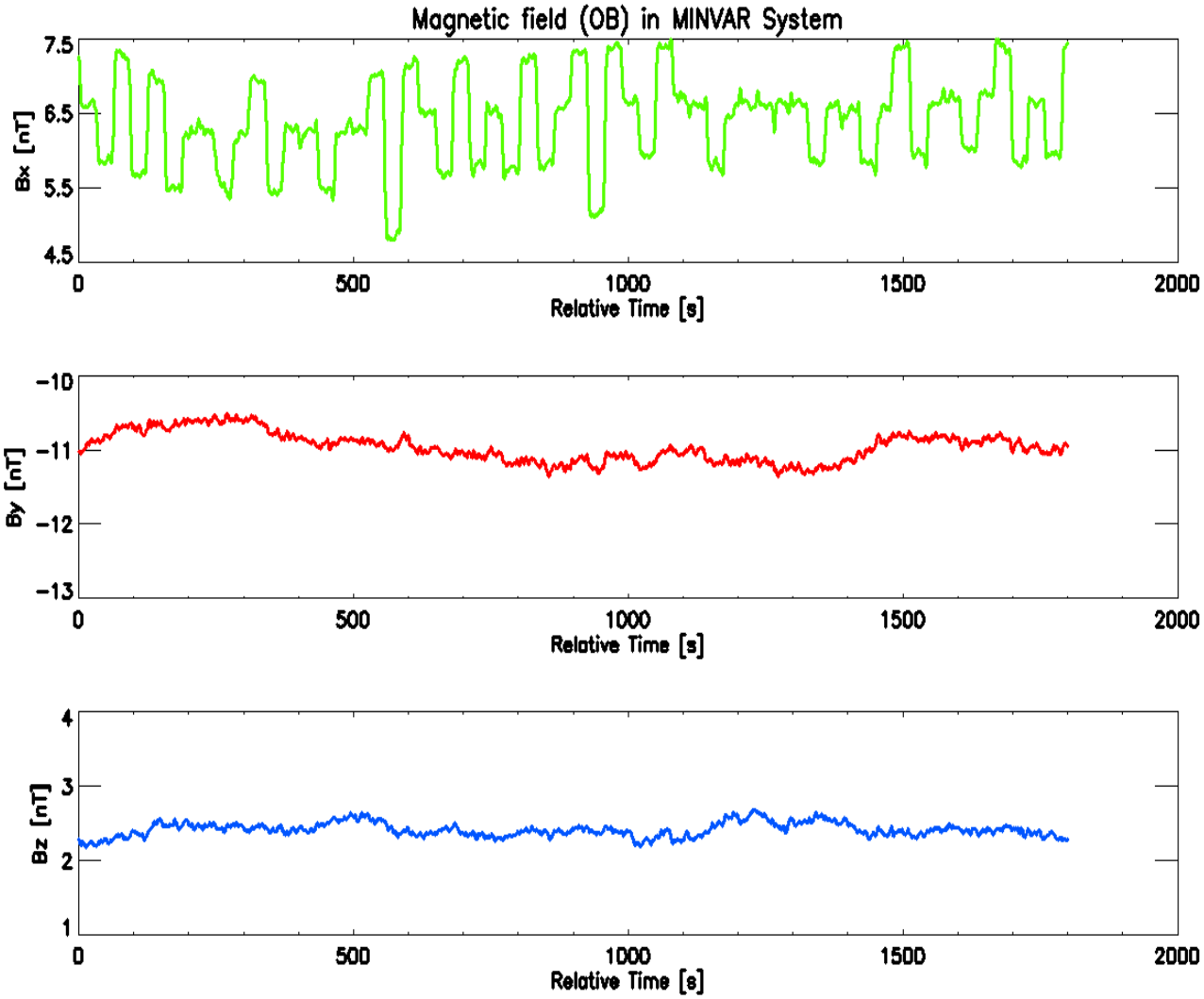

Figure 3: Disturbed signal rotated the Minimum Variance System

In the fourth panel the desired time series of "true" data is reconstructed. To do this the height of the jumps has to be computed individually for each jump. This height (level difference) is evaluated using short time averages of the last values of the level just before the jump and the average of the values just after the jump. With these data available it is possible to proceed step by step through the time series and to "flatten" all the infected levels. As the result the interrupted black–red time series is obtained.

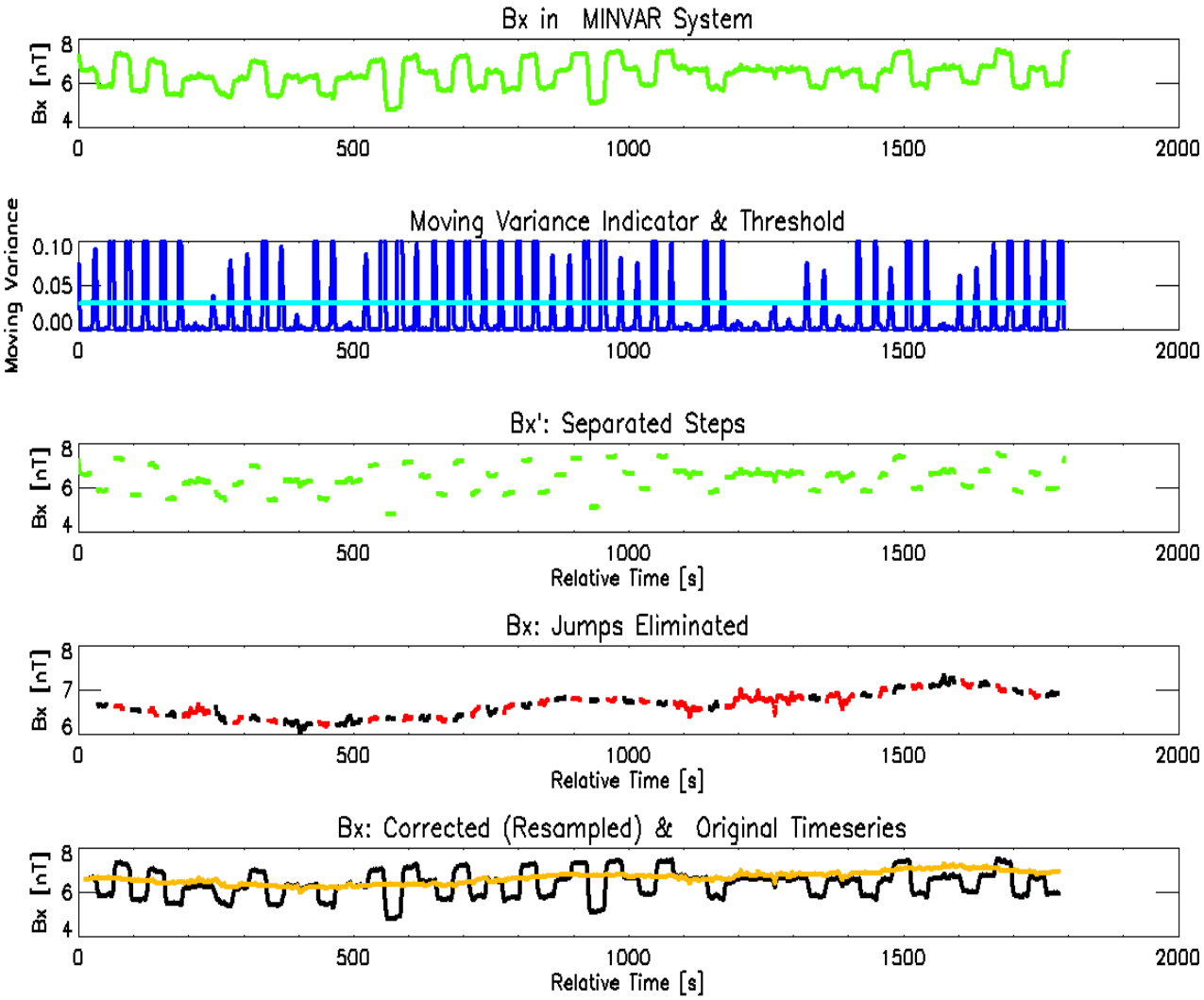

Figure 4: Processing of the heater disturbed Signal

The last step of the jump elimination can be seen in the bottom panels. The time gaps have been closed by resampling and interpolating the signal at the times of a jump. For a better comparison the original disturbed time series (black) and the improved signal (orange) are displayed.
At the very last processing step the corrected signal has to be rotated back from the minimum variance system to the original s/c frame. The result is shown in Figure 5.
The complete process can run quasi automatically to generate corrected PDS data.

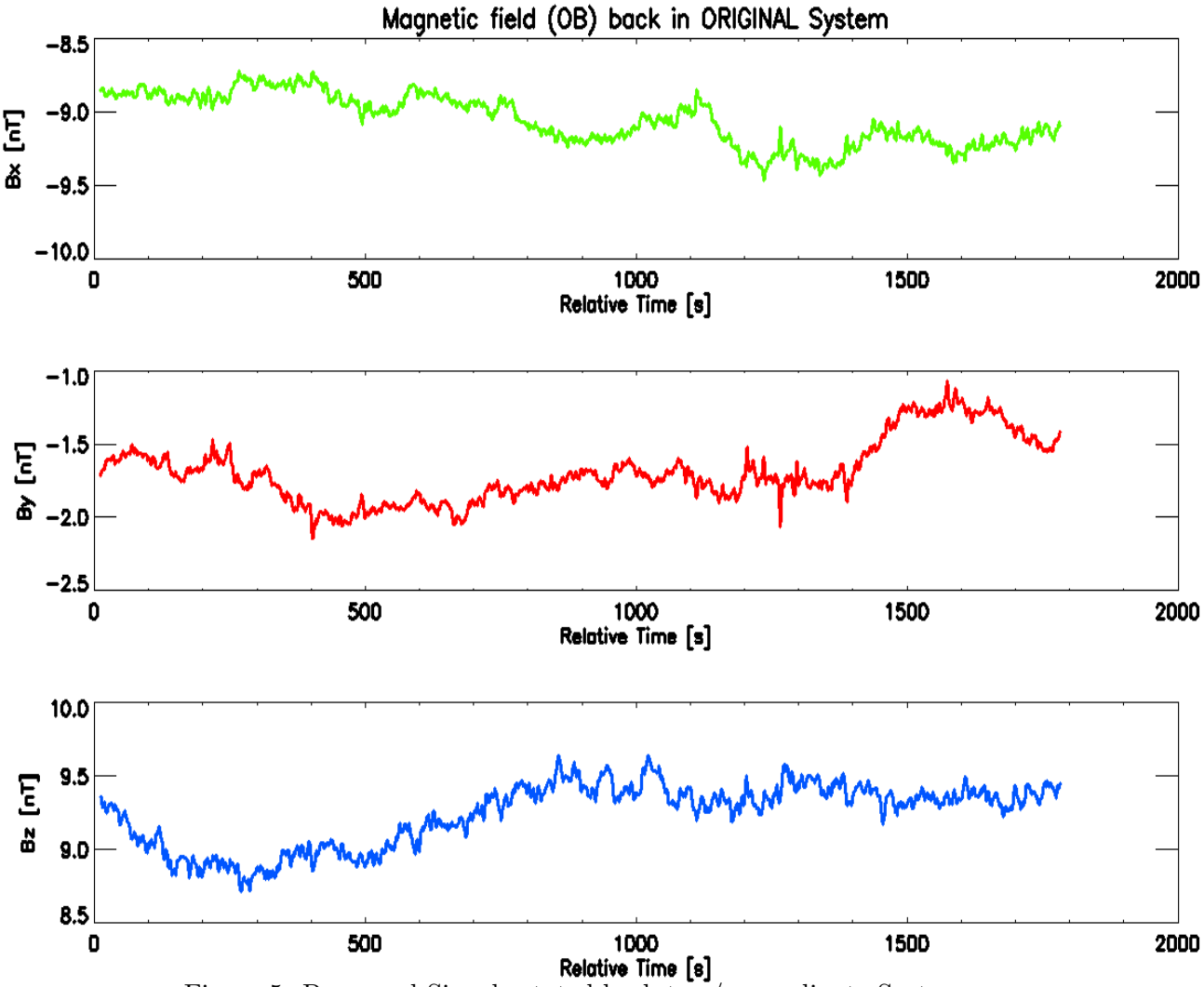

Figure 5: Processed Signal rotated back to s/c coordinate System

4.12.2 Heater Disturbance Elimination: Method 2

This method uses the doubtful advantage that the heater disturbances at the Lander magnetometer ROMAP were much higher than the ones at the location of the RPC-MAG sensor. Thus a disturbance identification and classification using the ROMAP instrument as a primary detector seems to be a promising mean. The correction procedure of RPC-MAG data using ROMAP data is visualized in the following diagram. The major feature of the process is a two stage procedure. At the first stage all disturbed times will be identified in the ROMAP data. Additionally the level of disturbance will be assigned to the actual activated heaters. In the second stage the RPC-MAG data will be purged using this advance information. The offset of data in the infected time intervals will be substituted by a new value according to the actual used heaters. Finally a purged timeseries is available.

It should be mentioned that LEVEL_K data are only needed for the ESB1 phase, as this was the only time were the Lander heaters were tested. After the release of the Lander at the Comet the heaters will not cause any orbiter disturbance anymore.

ROMAP

Identify number of activated heaters (1-6 at ESB1) and perform a coarse correction.

automatic process

⇒ ROMAP_LEVEL_1

↓

Eliminate time intervals with uncertain disturbance signatures (this regards almost only transient switch on/off events)

Loss of 0-6 data points in a interval of 30 s.

manual process

↓

Identification of activated Heaters (A, B, C, D, E, F) and specific Correction.

Identification: manual process
Correction: automatic process

⇒ ROMAP_LEVEL_2

↓

Elimination of long term time dependent trends in the disturbance signatures of individual heaters and any occurring combination of heaters.

manual process

⇒ ROMAP_LEVEL_3

→

RPC-MAG

Eliminate time shift between ROMAP and RPC-MAG data that might have occurred due to not compensated filter delays

automatic process

↓

Interpolation of ROMAP timestamps/data (still ±0.5 s after previous correction step)
Correction of RPC-MAG data.
Only two kinds of heaters (compartment & Battery) are distinguished (their signatures differ by about 20 nT at the location of the ROMAP sensor and are just separable at the RPC-MAG sensor position. The signatures of the other heaters are not resolvable at the RPC-MAG sensor location.)
The RPC-MAG correction has a higher data point loss rate during the switch on/off events - about 3 s-12 s are disturbed within a 30 s switch interval.

automatic process

↓

Add the time intervals where a correction is not possible (i.e ROMAP is switched off, TLM error, Sensor Saturation,...)

manual process

↓

Re-insertion of the original time differences between ROMAP and RPC-MAG. Interpolation of actual timestamps to original timestamps; eliminated points will not be taken into account.

automatic process

4.13 Generation of LEVEL_L Data

The LEVEL_L data represent Heater corrected data in ECLIPJ2000 coordinates. Thus they will be generated by rotating the LEVEL_K data from s/c-coordinates to the ECLIPJ2000 frame using either the ESA OASW S/W or SPICE kernels and S/W routines. The data are available in the following format.

Data	Description
TIME_UTC	UTC TIME OF OBSERVATION: YYYY-MM-DDTHH:MM:SS.FFFFFF
TIME_OBT	S/C CLOCK AT OBSERVATION TIME, SECONDS SINCE 00:00 AT 1.1.2003: SSSSSSSSS.FFFFF
POSITION_X	SPACECRAFT POSITION, X COMPONENT, ECLIPJ2000 VALUE IS GIVEN IN KILOMETER
POSITION_Y	SPACECRAFT POSITION, Y COMPONENT, ECLIPJ2000 VALUE IS GIVEN IN KILOMETER
POSITION_Z	SPACECRAFT POSITION, Z COMPONENT, ECLIPJ2000 VALUE IS GIVEN IN KILOMETER
BX	MAGNETIC FIELD X COMPONENT, CALIBRATED DATA, TEMPERATURE CORRECTED, ECLIPJ20000-COORDINATES,HEATER DISTURBANCE ELIMINATED, VALUE IS GIVEN IN NANOTESLA
BY	MAGNETIC FIELD Y COMPONENT, CALIBRATED DATA, TEMPERATURE CORRECTED, ECLIPJ2000-COORDINATES,HEATER DISTURBANCE ELIMINATED, VALUE IS GIVEN IN NANOTESLA
BZ	MAGNETIC FIELD Z COMPONENT, CALIBRATED DATA, TEMPERATURE CORRECTED, ECLIPJ2000-COORDINATES,HEATER DISTURBANCE ELIMINATED, VALUE IS GIVEN IN NANOTESLA
QUALITY	QUALITY FLAG, cf. EAICD chapter 3.3

A Abbreviations

Item	Meaning
a_i	Fit coefficients for temperature dependent offset
ADC	Analog Digital Converter
ATNR	Attitude file provided by FDT
$\underline{B}^c$	Magnetic calibration field generated by coil system
$\underline{B}^c_s$	Calibrated Magnetic field measured by sensor s
$\underline{B}^{off}$	Offset of the magnetometer [nT]
$\underline{B}^{off}_k$	Polynomial Fit coefficients for the sensor offset vs. temperature
$\underline{B}^m$	Measured magnetic field raw data, offset & residual field corrected [nT]
$\underline{B}^{or}$	$= \underline{B}^{off} + \underline{B}^{res}$, Offset + Residual field at CoC [enT]
$\underline{B}^r$	Magnetic field raw data
$B^r_{0^\circ}$	Magnetic raw data, measured in normal position (0°)[enT]
$B^r_{180^\circ}$	Magnetic raw data, measured in turned position (180°)[enT]
$\underline{B}^{res}$	Residual field of the coil system
e°C	Engineering degrees centigrade units
$\underline{B}^s_{ECLIP}$	Magnetic field measured by sensor s in ECLIPJ2000 coordinates
$\underline{B}^s_{s/c}$	Magnetic field measured by sensor s in s/c- coordinates
$\underline{B}^s_{URF}$	Magnetic field measured by sensor s in Instrument coordinates
c_0, c_1, c_2, c_3	Fit coefficients of the sensor thermistor
CoC	Center of Coil system
CSO	Cometo-centric solar orbital coordinates
DDS	Data Distribution System
DPU	Digital Processing Unit
enT	Engineering NanoTesla units applicable after nominal conversion of ADC counts
ESB	Earth Swing by
$\underline{\underline{F}}$	$=\underline{\underline{SOR}}$, Transfer Matrix
FGM	Fluxgate Magnetometer
FDT	Flight Dynamics Team of ESOC
FM	Flight Model
FS	Flight Spare Unit
FSDPU	Flight Spare Digital Processing Unit
GSE	Geocentric Solar Ecliptic coordinates
HGA	High Gain Antenna
HK	Housekeeping data
i	component x | y | z
IB	Inboard Sensor
$\underline{\underline{K}}$	Geometric correction Matrix for alignment angles
k_i	Geometric correction factors for sensitivities
λ, μ, ν	Euler rotation angles
LAP	RPC instrument: Langmuir Probe

Item	Meaning
MCF	Magnetic calibration Facility
MSO	Mars centered solar orbital coordinates
$\underline{\underline{O}}$	Orthogonalisation matrix
OASW	Orbit and Attitude Software, provided by ESA
OB	Outboard Sensor
OBDH	Onboard Data handling system
$\underline{\underline{\omega}}$	$= \underline{\underline{O}}^{-1}$, Inverse orthogonalisation matrix
ORER	Orbit and Position file (related to EARTH) provided by FDT
ORHR	Orbit and Position file (related to SUN) provided by FDT
ORMR	Orbit and Position file (related to MARS) provided by FDT
$P_3(T)$	3rd order Fit-polynomial of Temperature
$p_{s,k,i}$	fit coefficient of sensor s, order k and component i
$\underline{\underline{\phi}}$	$= \underline{\underline{F}}^{-1}$, Inverse Transfer Matrix
PIU	Power interface unit
$\underline{\underline{R}}$	Rotation matrix of sensor vs. coil system
$\underline{\underline{\rho}}$	$= \underline{\underline{R}}^{-1}$, Inverse rotation matrix
$\underline{\underline{S}}$	Sensitivity matrix
s	Sensor index $s = \{\text{IB} \mid \text{OB}\}$
$\underline{\underline{\sigma}}$	$= \underline{\underline{S}}^{-1}$, Inverse sensitivity matrix
$\sigma_{k,i}$	Polynomial Fit coefficient for sensitivity vs. temperature. Coefficient of order k for the sensor component i
T	Temperature
T_i	Temperature of measurement i
TLM	Telemetry
T_s^O	Additional Temperature offset of sensor Thermistor s
T_s^c	Temperature of sensor s, calibrated data [°C]
T_s^r	Temperature of sensor s, raw data [e°C]
s	Sensor IB | OB
s/c	spacecraft
URF	Unit Reference Frame, Instrument–Coordinates
$U_{\text{T, IB}}$	IB–Temperature data [V], measured
$U_{\text{T,OB}}$	OB–Temperature data [V], measured
uvw	Instrument coordinate axes
ξ_{ij}	Temperature dependent alignment angle (ij component)
$\xi^0_{k,ij}$	Polynomial Fit coefficient for misalignment angle vs. temperature. Coefficient of order k for the angle ij

B Offset Correction Algorithm for the "After Hybernation Phase"

B.1 Correction of OB data

```
OFFSET_JUMP= [['2004-01-01T00:00:00',  '2012-01-01T00:00:00'],$
  ['2014-01-01T00:00:00',  '2014-03-27T05:00:00'],$
  ['2014-04-16T22:00:00',  '2014-04-17T07:00:00'],$
  ['2014-05-09T15:00:00',  '2014-05-20T11:00:00'],$
  ['2014-05-23T14:00:00',  '2014-06-03T10:00:00'],$
  ['2014-06-06T03:00:00',  '2014-06-17T10:00:00'],$
  ['2014-06-20T02:00:00',  '2014-07-01T08:00:00'],$
  ['2014-07-04T02:00:00',  '2014-07-08T08:00:00'],$
  ['2014-07-11T02:00:00',  '2014-07-15T02:00:00'],$
  ['2014-07-18T02:00:00',  '2014-07-22T02:00:00'],$
  ['2014-07-25T02:00:00',  '2014-09-13T03:00:00'],$
  ['2014-09-15T14:00:00',  '2014-10-01T15:00:00'],$
  ['2014-10-02T08:00:00',  '2014-10-30T02:00:00'],$
  ['2014-10-30T04:00:00',  '2014-11-12T08:35:00'],$
  ['2014-11-12T08:35:00',  '2014-11-13T00:00:00'],$
  ['2014-11-13T00:00:00',  '2015-01-14T09:00:00'],$
  ['2015-01-17T00:00:00',  '2015-01-18T10:00:00'],$
  ['2015-01-18T11:00:00',  '2015-02-14T13:10:00'],$
  ['2015-02-14T13:10:00',  '2018-01-01T00:00:00']]

JUMP_SUM_OB_X =    [0.000,$
  -0.6443,$
  -0.6443,$
  0.5954,$
  -2.0896,$
  -1.3826,$
  0.6297,$
  -0.1665,$
  -0.5286,$
  -0.4732,$
  -1.4364,$
  9.0744,$
  8.4542,$
  8.2876,$
  -7.8000,$
  -8.5240,$
  -8.5240,$
  -8.5240,$
```

```
  -4.52]



JUMP_SUM_OB_Y =   [0.000,$
  0.7116,$
  -1.2884,$
  0.6396,$
  -3.3906,$
  0.1758,$
  4.5775,$
  7.3484,$
  7.3515,$
  -3.6564,$
  -0.2041,$
  12.3533,$
  14.9331,$
  13.2751,$
  8.9000,$
  9.2652,$
  9.2652,$
  9.2652,$
  25.26]



JUMP_SUM_OB_Z =  [0.000,$
  -2.2752,$
  1.7248,$
  3.3307,$
  1.8250,$
  0.7866,$
  1.4086,$
  1.0691,$
  -1.7854,$
  -0.0780,$
  -0.6965,$
  -5.1818,$
  -2.3597,$
  -4.4664,$
  -15.7000,$
  -9.5247,$
  -9.5247,$
  -9.5247,$
```

```
 -5.52]


 n_offs=n_elements(offset_jump(0,*))

 for III=0,n_offs-1 do begin
  index_jump=where(btime(*) ge offset_jump[0,III]  and btime(*) le offset_jump[1,III])
  if index_jump(0) ne -1 then begin
    B(0,index_jump) = B(0,index_jump) -JUMP_SUM_OB_X[III]
    B(1,index_jump) = B(1,index_jump) -JUMP_SUM_OB_Y[III]
    B(2,index_jump) = B(2,index_jump) -JUMP_SUM_OB_Z[III]
  endif
  endfor

endif
```

B.2 Correction of IB data

```
OFFSET_JUMP= [['2004-01-01T00:00:00',  '2012-01-01T00:00:00'],$
  ['2014-01-01T00:00:00',  '2014-03-27T05:00:00'],$
  ['2014-04-16T22:00:00',  '2014-04-17T07:00:00'],$
  ['2014-05-09T15:00:00',  '2014-05-20T11:00:00'],$
  ['2014-05-23T14:00:00',  '2014-06-03T10:00:00'],$
  ['2014-06-06T03:00:00',  '2014-06-17T10:00:00'],$
  ['2014-06-20T02:00:00',  '2014-07-01T08:00:00'],$
  ['2014-07-04T02:00:00',  '2014-07-08T08:00:00'],$
  ['2014-07-11T02:00:00',  '2014-07-15T02:00:00'],$
  ['2014-07-18T02:00:00',  '2014-07-22T02:00:00'],$
  ['2014-07-25T02:00:00',  '2014-09-13T03:00:00'],$
  ['2014-09-15T14:00:00',  '2014-10-01T15:00:00'],$
  ['2014-10-02T08:00:00',  '2014-10-30T02:00:00'],$
  ['2014-10-30T04:00:00',  '2014-11-12T08:35:00'],$
  ['2014-11-12T08:35:00',  '2014-11-13T00:00:00'],$
  ['2014-11-13T00:00:00',  '2015-01-14T09:00:00'],$
  ['2015-01-17T00:00:00',  '2015-01-18T10:00:00'],$
  ['2015-01-18T11:00:00',  '2015-02-14T13:10:00'],$
  ['2015-02-14T13:10:00',  '2018-01-01T00:00:00']]



JUMP_SUM_IB_X =[0.000,$
```

```
  0.4322,$
  0.4322,$
  2.3403,$
  0.0904,$
  0.0904,$
  0.2279,$
  3.0616,$
  3.0616,$
  1.1037,$
  -1.0137,$
  2.1689,$
  2.1689,$
  2.1689,$
  -7.5000,$
  -8.7412,$
  -8.7412,$
  -8.7412,$
  -13.74]


JUMP_SUM_IB_Y =[0.000,$
  0.8046,$
  1.9944,$
  12.9253,$
  6.7833,$
  0.7486,$
  4.3631,$
  16.1721,$
  8.0264,$
  3.2022,$
  -9.8093,$
  8.6587,$
  4.3783,$
  4.3783,$
  3.8000,$
  7.5576,$
  7.5576,$
  7.5576,$
  -0.4424]


JUMP_SUM_IB_Z =[0.000,$
  -0.4443,$
  -0.7393,$
  -4.5484,$
  -4.5484,$
```

```
-2.0144,$
-2.0144,$
-4.1340,$
-3.1969,$
-3.1718,$
1.1286,$
-6.5916,$
-6.5916,$
-12.3560,$
-13.3000,$
-19.2265,$
-19.2265,$
-19.2265,$
 0.7735]
```